

INFORMATION TO USERS

This was produced from a copy of a document sent to us for microfilming. While the most advanced technological means to photograph and reproduce this document have been used, the quality is heavily dependent upon the quality of the material submitted.

The following explanation of techniques is provided to help you understand markings or notations which may appear on this reproduction.

1. The sign or "target" for pages apparently lacking from the document photographed is "Missing Page(s)". If it was possible to obtain the missing page(s) or section, they are spliced into the film along with adjacent pages. This may have necessitated cutting through an image and duplicating adjacent pages to assure you of complete continuity.
2. When an image on the film is obliterated with a round black mark it is an indication that the film inspector noticed either blurred copy because of movement during exposure, or duplicate copy. Unless we meant to delete copyrighted materials that should not have been filmed, you will find a good image of the page in the adjacent frame.
3. When a map, drawing or chart, etc., is part of the material being photographed the photographer has followed a definite method in "sectioning" the material. It is customary to begin filming at the upper left hand corner of a large sheet and to continue from left to right in equal sections with small overlaps. If necessary, sectioning is continued again—beginning below the first row and continuing on until complete.
4. For any illustrations that cannot be reproduced satisfactorily by xerography, photographic prints can be purchased at additional cost and tipped into your xerographic copy. Requests can be made to our Dissertations Customer Services Department.
5. Some pages in any document may have indistinct print. In all cases we have filmed the best available copy.

**University
Microfilms
International**

300 N. ZEEB ROAD, ANN ARBOR, MI 48106
18 BEDFORD ROW, LONDON WC1R 4EJ, ENGLAND

1316999

AGNEW, JAMES DENNIS
SEISMICITY OF THE CENTRAL ALASKA RANGE,
ALASKA, 1904 - 1978.

UNIVERSITY OF ALASKA, M.S., 1980

COPYR. 1980 AGNEW, JAMES DENNIS

University
Microfilms
International

300 N. ZEEB RD., ANN ARBOR, MI 48106

PLEASE NOTE:

In all cases this material has been filmed in the best possible way from the available copy. Problems encountered with this document have been identified here with a check mark .

1. Glossy photographs or pages _____
2. Colored illustrations, paper or print _____
3. Photographs with dark background _____
4. Illustrations are poor copy _____
5. Pages with black marks, not original copy _____
6. Print shows through as there is text on both sides of page _____
7. Indistinct, broken or small print on several pages
8. Print exceeds margin requirements _____
9. Tightly bound copy with print lost in spine _____
10. Computer printout pages with indistinct print _____
11. Page(s) _____ lacking when material received, and not available from school or author.
12. Page(s) _____ seem to be missing in numbering only as text follows.
13. Two pages numbered _____. Text follows.
14. Curling and wrinkled pages _____
15. Other _____

**University
Microfilms
International**

SEISMICITY OF THE CENTRAL ALASKA RANGE, ALASKA, 1904 - 1978

A
THESIS

Presented to the Faculty of the
University of Alaska in partial fulfillment
of the Requirements
for the Degree of

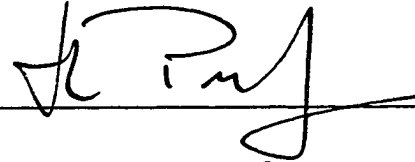
MASTER OF SCIENCE

James D. Agnew, B.A.
Fairbanks, Alaska
August, 1980

© Copyright, 1980, James D. Agnew

SEISMICITY OF THE CENTRAL ALASKA RANGE, ALASKA, 1904 - 1978

RECOMMENDED:




N. N. [unclear]

D. B. [unclear]


Chairman, Advisory Committee


Division Head

APPROVED:


Dean of College of Environmental Sciences

6-16-80
Date


Vice Chancellor for Research and Advanced Study

June 18, 1980
Date

ABSTRACT

Seismic evidence indicates that the Aleutian-Alaskan Benioff zone extends northeasterly through Cook Inlet to the central Alaska Range, ending at 64.1° North latitude, 148.0° West longitude, 45 km north of the Hines Creek strand of the Denali Fault. The direction of strike of the northeast end of the Benioff zone is $N52^{\circ}E$, indicating a 35° bend in the subducting plate in the Yentna River region. The seismicity of this area, one bounded by 62° to 64.05° North latitude, 145.8° to 156° West longitude, is higher than that of the Fairbanks area to the north and much higher than the area to the east. The subducting Pacific plate enters the area from the southeast at dip angle 15° to 20° , and then dips more steeply at 45° to 50° under the central Alaska Range, where it reaches a depth of 150 km.

ACKNOWLEDGMENTS

I express my sincere thanks to Professor T. Neil Davis for acting as my advisor. His comments and suggestions were extremely helpful. I also thank Professors N. N. Biswas, H. Pulpan and D. B. Stone who were members of my graduate committee. Their advice and constructive criticism are appreciated. Steven Estes and Dianne Marshall helped me greatly with computer work. I also thank Larry Gedney and the late Sir Edward Bullard for helpful advice and encouragement. I thank Paula Jones for typing the manuscript. This study was supported by USGS Contract 14-08-0001-16823 and by State of Alaska funds appropriated to the Geophysical Institute.

TABLE OF CONTENTS

	<u>Page</u>
Title Fly	1
Title Page	2
Abstract	3
Acknowledgments	4
Table of Contents	5
List of Figures	6
List of Tables	8
1. Introduction	9
2. Regional Tectonic Setting	10
3. Sources and Data Reduction Methods	14
4. Presentation of Data	22
4.1 General Seismicity	22
4.2 Energy Release and Number of Events per Month	26
4.3 The Benioff Zone	27
4.4 Strain Release	32
5. Discussion	35
6. Conclusions	42
Suggestions for Future Seismic Work	43
Figures	45
Tables	70
Bibliography	81

LIST OF FIGURES

<u>Figure</u>	<u>Subject</u>	<u>Page</u>
1	Boundaries of thesis area	45
2	Known faults within study area	46
3	Location of seismometer stations	47
4	All earthquakes from Aug. 1904 - Aug. 1967	48
5	All earthquakes from Sept. 1967 - April 1974	49
6	All earthquakes from May 1974 - Dec. 1978	50
7	Cumulative Magnitude plot, Sept. 1967 - April 1974	51
8	Cumulative Magnitude plot, May 1974 - Dec. 1978	52
9	Number of Earthquakes per month, Sept. 1967 - Dec. 1978..	53
10	Energy Release per month, Sept. 1967 to Dec. 1978	54
11	Vertical plane view of all events from May 1974 to	55
	December 1978 looking N17°E	
12	Vertical plane view of all events from May 1974 to	56
	December 1978 looking N44°E	
13	Vertical plane view of all earthquakes from May 1974	57
	to December 1978 looking N46°W	
14	Map view of Best-fit (constrained) earthquakes in	58
	the study area	
15	Vertical plane view of all constrained earthquakes	59
	looking N52°E	
16	Vertical plane view of all constrained earthquakes	60
	looking N38°W	

<u>Figure</u>	<u>Subject</u>	<u>Page</u>
17	Stereopairs of earthquakes in the Benioff Zone showing a three-dimensional view along strike and normal to strike	61
18	Map view of the 75-, 100-, and 125-km depth contours .. of the top of the Benioff zone	62
19	Strain Release for all earthquakes having focal depths of 30 km or less, Sept. 1967 - Dec. 1978	63
20	Strain Release for all earthquakes having focal depths greater than 30 km, Sept. 1967 - Dec. 1978	64
21	Strain Release for all earthquakes regardless of depth, Sept. 1967 - Dec. 1978	65
22	All earthquakes of magnitude 3.5 or greater from 1904 to August, 1967 near the proposed Susitna dam sites	66
23	All earthquakes of magnitude 3.5 or greater from Sept. 1967 to April 1974 near the proposed Susitna dam sites	67
24	All earthquakes of magnitude 3.5 or greater from May 1974 to Dec. 1978 near the proposed Susitna dam sites	68
25	Relative sizes of earthquakes on Figs. 21, 22 and 23 ..	69

LIST OF TABLES

<u>Table</u>	<u>Subject</u>	<u>Page</u>
1	All earthquakes of M = 6.0 or greater	70
2	List of all stations used in study	71
3	Quality of earthquake locations during the epoch May 1974 to December 1978	72
4	Velocity Model Used For Group III Earthquakes, May 1974 to December 1978	74
5	Comparison of Depths using P, then P and S First Motion	75
6	Average Depth of Geophysical Institute Locations Compared to NOAA Solutions	76
7	Sliding Window of 200 events and b-slopes	77
8	All earthquakes of magnitude 3.5 or greater within approximately 50 km of the proposed Susitna dam sites	79

1. INTRODUCTION

Earthquakes have been felt in central Alaska at least since historical records have been kept. Some of the largest of the early events are documented by Davis and Echols (1962). Prior to the installation of a seismograph at College, Alaska (COL) in 1935, only recordings made at distant stations were available to locate the epicenters and focal depth of earthquakes in central Alaska. With such data, Richter (1958) and Davis (1964) produced generalized maps of Alaskan seismicity showing shallow- and intermediate-depth earthquakes extending from the Aleutian Islands north to interior Alaska. A narrow zone of intermediate-depth seismicity was described by Tobin and Sykes (1966) as extending from the Alaska Peninsula to the northern boundary of the Alaska Range, some 250 km northeast of the last active volcano, Mt. Spurr. Since Tobin and Sykes' study, another volcano displaying Recent activity, Hayes, has been discovered at the foot of Mt. Gerdine, approximately 90 km north of Mt. Spurr (Miller and Smith, 1976). Tobin and Sykes (1966) could not associate shallow-depth earthquakes with known faults, but they noted that several earthquakes may have occurred on or near the Denali Fault, which runs through the center of the arcuate Alaska Range.

With the inception of the University of Alaska seismic network and other networks to the south, in 1964, earthquakes could be more accurately located in central Alaska. As data from these networks accumulated, new studies became possible. A major influence upon these studies has been the emergence of the theory of plate tectonics. In

essence, it is now believed that the underlying cause of the seismic activity in central Alaska is the subduction of the Pacific plate as it spreads northward from the East Pacific Rise (Isacks et al., 1968; Tobin and Sykes, 1968). The downgoing Pacific plate extends into interior Alaska (VanWormer et al., 1973; Davies and Berg, 1973; Biswas, 1973) through Cook Inlet and the Susitna lowlands to the Alaska Range, although its northernmost limit, until now, has not been clearly resolved.

One of the purposes of this study is to outline the strike, maximum depth and lateral extent of the Benioff zone (the dipping earthquake zone) in the central Alaska Range, and to locate its northernmost extent using the latest available earthquake data. Another is to better define the general seismicity of part of central Alaska bounded by 62° to 64.05° North latitude, 145.8° to 156° West longitude, which includes all of Mt. McKinley National Park, most of the central Alaska Range and the Talkeetna Mountains, and part of the Kuskokwim Mountains (Figure 1). An attempt is made to relate the pattern of strain-release in the area with the known fault structure and the regional tectonic setting as it is presently understood. It happens that this area is of special current interest because of two proposed hydroelectric dam sites on the Susitna River, so some discussion is given of the seismicity as it relates to the proposed sites.

2. REGIONAL TECTONIC SETTING

The great fault system running through the Alaska Range was simultaneously reported by St. Amand (1954) and Sainsbury and Twenhofel

(1954). St. Amand called it the Denali Fault and hypothesized that it is of major tectonic significance (1957), as did Twenhofel and Sainsbury (1958). This right-lateral (dextral) strike-slip fault extends for over 2,100 km in an arc from the Yukon Territory to the Bering Sea, displaying scissoring reversals of vertical displacement in a well-defined lineament or trough cutting through the mountains, occupied in places by glaciers (Stout et al., 1973). The Denali Fault is actually a system of many faults including the Farewell Fault, McKinley and Hines Creek strands, and the Shakwak Valley fault (Figure 2). Descriptions of these and smaller segments are given by Cady et al. (1955), Grantz (1966) and Brogan et al. (1975). All of these faults are of the right-lateral strike-slip variety. The Denali Fault system separates Precambrian and Paleozoic crystalline metamorphic rocks of the Yukon-Tanana complex to the north from Paleozoic and Mesozoic bedded and volcanic sedimentary rocks to the south (Stout, 1965; Smith, 1971; Smith and Lanphere, 1971).

The eastern part of the Denali Fault is a transform fault (Tobin and Sykes, 1968) caused by the thrusting of the Pacific Ocean sea floor beneath the mainland of southern Alaska. Much evidence has accumulated for large dextral slip along the Denali Fault; the largest estimate is 415 km (Forbes et al., 1973, 1974; Hickman et al., 1978) since the Late Cretaceous Period. South-up vertical movement at Mt. McKinley is estimated at 3 km since the Mid-Tertiary (Reed and Lanphere, 1974). This motion has continued to the present, as is shown by recent north-facing scarps up to 2.5 m high (Grantz, 1966). Estimates of dextral slip rates range from 0.5 cm/yr (Stout et al., 1973) up to 3.3 cm/yr

(Richter and Matson, 1971), but Reed and Lanphere (1974) suggest that the slip rate may be variable along the fault trace. Lack of offset in some 143-year old moraines (Stout et al., 1973) and some alluvial fans (Hickman and Craddock, 1973) on the Denali Fault trace led Reed and Lanphere (1974) to postulate that the present day fault activity may not be at its average Holocene slip rate.

No active slippage could be ascertained for the McKinley Strand over a two-year period using a geodetic network (Page and Lahr, 1971) although Page (1972) concludes that there may have been up to 14 cm of dextral slip near the Alaska Railroad between 1942 and 1970. Due to the strain release associated with the 1964 Prince William Sound earthquake ($M = 8.3$) to the southeast, some authors believe the Denali Fault may be locally locked (Page and Lahr, 1971; Page, 1972). Shear strain accumulation is below detectable levels on the fault (Savage, 1975), but Forbes et al. (1976) conclude that the Denali Fault can be considered "active" between McKinley Park and the Denali-Totschunda fault juncture.

The only other major fault in the study area is the Iditarod-Nixon Fork Fault (Figure 2), which is also dextrally offset with some evidence of thrusting both to the north and south along its 500 km length (Grantz, 1966). Grantz estimates dextral offset at between 35 and 110 km in Cretaceous rocks and considers the fault to be active.

Of the earthquakes in south-central Alaska, one deserves special mention. It is the first and largest earthquake ever reported as occurring in the area studied in this thesis project. It took place on August 27, 1904, and had a magnitude estimated at $7\frac{3}{4}$ to $8\frac{1}{4}$ (Davis

and Echols, 1962; Meyers, 1976). The location, given to the nearest degree, was 64° North latitude, 151° West longitude. This estimate was made from seismic stations in California (Berkeley, Pasadena) and could be in error by as much as 100 km. Ground motion was widely felt; a newspaper account from St. Michael, near 63.5°N , 162°W , reads as follows:

Severe Earthquake Occurs at St. Michael--Special to the Nome News via Telegraph. St. Michael, August 29.--This place was visited by a severe earthquake at 10:55 o'clock Saturday morning lasting for more than five minutes. Everything was violently disturbed while the shock lasted and a number of people were made seasick from the movement of the ground. Beyond the fear engendered in the hearts of everyone here, there was no damage done.

Nome Semi-Weekly News
Tues., Aug. 30, 1904.

Although most felt reports were from Rampart, near 65.5°N , 150.2°W , which is much closer to the estimated epicentral location, the intensity was not as great as at St. Michael:

Rampart Shaken by Earthquake - Duration less than a minute and no damage done - At 11:30 o'clock last Saturday, Rampart experienced a distinct shock of earthquake. The disturbance was much more marked on Second Avenue and in that part of town lying along the foot of the hill than on First Avenue and along the river front. On Second Avenue buildings swayed and cracked and inmates ran out in alarm. On First Avenue in some instances the shock was not felt even by people on the sidewalk. It continued slightly less than a minute and was most violent just after its beginning and just before its close. Most people in from the creeks say the shock was not felt there. Fred Bevere, at his Hunter Creek claim, thought he felt a slight quake, but afterwards concluded he was mistaken.

Yukon Valley News
Rampart, Aug. 31, 1904.

Another news item, which may or may not be associated with the earthquake, reads as follows:

A committee of public-spirited citizens headed by Dr. Gibbons repaired the fractured and dislocated sidewalks of the camp last Wednesday last. They have the thanks of the community.

Alaska Forum
Rampart, Sat., Oct. 15, 1904.

No newspapers from that time period could be found for the Fairbanks area in either the Fairbanks city library or the University of Alaska library, and the Daily News-Miner did not have back copies of the Fairbanks News from that time period. Nevertheless, it seems improbable that a major earthquake only 170 km southwest of Rampart could go unnoticed by some Rampart residents unless the given epicentral location is greatly in error.

Seismic activity since the August 27, 1904 earthquake has been less severe. One magnitude-7.4 event took place July 7, 1912, but the given location of 64°N, 147°W is probably no more accurate than that of the 1904 earthquake. Thirteen earthquakes in the study area have been given estimated magnitudes of 6.0 or greater, in addition to the two already mentioned. Table 1 lists all earthquakes with a magnitude of 6.0 or greater within the boundaries of the study area. Not included is a magnitude-7.3 earthquake which occurred on October 16, 1947. Of four published epicenter locations for this event, three are outside the northern boundary of 64.05°N (BSSA, vol. 38; St. Amand, 1948; Int'l Seismol. Summary, 1947), and one is given as 63.8°N, 148.1°W (Jesuit Seismol. Rpt., BSSA, vol. 38).

3. SOURCES AND DATA REDUCTION METHODS

The earthquake data used in this study came from two sources. One

source is the seismic network maintained by the Geophysical Institute at the University of Alaska, Fairbanks. This network has grown from one station installed near the McKinley Park hotel in 1964 to approximately forty stations at the time of this writing. The data obtained from this network are stored on a computer tape.

The second source of data is a listing of earthquakes on the National Oceanographic and Atmospheric Administration (NOAA) computer tape (Meyers, 1976). Most of these earthquakes have magnitudes of 3.5 or greater.

The station locations used in this study are shown in Figure 3; information on each station is presented in Table 2. The Geophysical Institute records some of the NOAA stations, and many of the earthquakes located by the Institute incorporate P-wave first-motion times from both the Institute network and the NOAA Tsunami Warning Network in Palmer, Alaska.

The two data sets were combined on a computer file, and duplications were identified through a sorting procedure and checked by hand. The Geophysical Institute data were used for all duplicates. However, 192 earthquakes listed on the NOAA tape had no corresponding Institute listings. These 192 earthquakes remained in the file. After the removal of duplicates, there were 7,017 earthquakes in the file. These constituted the total of all recorded and located shocks from August 27, 1904 to December 31, 1978.

Each earthquake listing contains the date and origin time (Greenwich Mean Time) of the event, latitude and longitude of the epicenter,

depth to focus in km, and Richter local magnitude (M_L). Later earthquake listings also include such parameters as number of stations used to locate the earthquake, root-mean-square travel time error (RMS), horizontal error in km (ERH), depth error in km (ERZ), largest azimuthal angle between stations in degrees (GAP), and distance to nearest station in km (DMIN).

The 7,017 earthquakes in the study area from 1904 to 1978 have been divided into three temporally determined groupings corresponding to identifiable epochs of differing quality in the earthquake locations.

Group I consists of 170 earthquakes occurring from August 1904 to September 1967 (Figure 4). No error estimates are given for latitude, longitude, depth or RMS errors. Both the locations and magnitudes of these 170 earthquakes can be considered as only approximate.

Group II is comprised of 4,263 earthquakes occurring between October 1967 through April 1974 (Figure 5). During this time period the Geophysical Institute used a computer program, EPICNTR, based on a velocity model of several layers over a half-space, to locate all events. The program gave epicenter locations to the nearest tenth of a degree, focal depths in discrete values from the tables of Herrin (1968), and RMS residuals which are defined as

$$\text{RMS} = \sqrt{\frac{\sum (\sigma - c)^2}{n}} \quad (1)$$

where σ is the observed travel time, c is the calculated travel time, and n is the number of arrivals used. The largest earthquake in Group

II was of magnitude 5.6; it occurred on November 3, 1970, at 62.0°N, 151.2°W (NOAA location) at a depth of 70 km.

Group III contains 2,584 earthquakes occurring from May 1974 through December 1978 (Figure 6). These earthquakes were located with the computer program HYP071 (Lee and Lahr, 1971; 1975). The accuracy of hypocenter location of Group III earthquakes is greatly improved over those of Group II. HYP071 gives error estimates including RMS residuals, horizontal error (ERH), and vertical error (ERZ), and also gives the parameters GAP (largest azimuthal angle between stations) and DMIN (epicentral distance to nearest station). The largest earthquake during this time period was of magnitude 5.4 on May 18, 1975, at 63°10.2'N, 150°15.8'W at depth 106 km (NOAA location).

The NOAA tape also lists a magnitude 5.4 earthquake in the study area on October 18, 1975. A check with Geophysical Institute data and the International Seismological Commission catalog revealed that all P-wave first motions scaled correspond to a nuclear blast in Russia at Novaya Zemlya. Thus, this shock was dropped from the list.

Although Groups I and II (1904-1974) contain useful and important information (see VanWormer et al., 1974; Davies, 1975), this thesis is mainly concerned with the more accurate data from Group III (1974-1978). Table 3 gives the quality of Group III earthquakes in percentages meeting certain levels of error in RMS residuals, ERH and ERZ. Also shown are the percentages of earthquakes for different GAP's, ratios of DMIN to focal depth, the number of stations used, and the depth distribution of all events.

It is evident that horizontal (epicentral) control is much better than depth control, since approximately 90% of the Group III earthquakes have horizontal error estimates of 25 km or less, whereas only 74% of the earthquakes have vertical error estimates of 25 km or less (Table 3). Huang (1979) has shown that the quality of epicentral location decreases when the GAP parameter becomes greater than 160° . As Table 3 shows, only about 28% of the earthquakes have a GAP less than 160° , making it the harshest constraint for sorting out earthquakes having the best locations. Approximately half of the earthquakes have a DMIN/DEPTH ratio of 5 or less, indicating that a major proportion of events occurred near the seismometer stations. Fully half of the events have computed depths of 30 km or less, although this bias may be due in part to the plane-layered velocity model assumed (Table 4).

The accuracy of earthquake magnitudes must be considered in studies of seismicity and energy release. Richter local body-wave magnitude, M_L , is determined at the Geophysical Institute by the following equation:

$$M_L = \log \left[A \cdot \frac{W.A.(f)}{G(f)} \right] - \log A_0 \quad (2)$$

in which A is one half the maximum peak-to-peak amplitude on the seismogram trace in mm, $W.A.(f)$ is the gain or magnification of ground motion at frequency f on a Wood-Anderson horizontal seismometer, $G(f)$ is the gain or magnification at frequency f of the vertical-component seismometer used, and A_0 is the trace amplitude, in mm, for a "standard"

earthquake which is a function of the distance to the epicenter determined from tables given by Richter (1958).

Errors in magnitude estimation are introduced by several factors:

1. Human reading errors in peak-to-peak amplitude (approximately ± 1.0 mm) and errors in epicentral distance determination (approximately ± 10 km). Their effect on magnitude estimation is generally very small.
2. Physical conditions of the earth along the ray path, generally assumed to be an isotropic homogeneous medium with overlying layers of differing velocity. Deviations from the assumed structure can affect the distance and depth estimates of the earthquake focus, and thus the magnitude estimate.
3. Ground conditions at the recording site, usually assumed to be solid rock. Amplitudes on the earthquake trace may be much greater if the seismometer is placed on alluvium or unconsolidated soils.
4. Possible directional effects of energy transmission due to fault orientation and slip direction. Several seismometers oriented around the epicenter generally reduce the directional effect.
5. Errors in calibration of the seismometers. A difference of a factor of two in the calibration will produce a magnitude error of ± 0.3 units.
6. Use of Richter's California attenuation scale on Alaskan data may produce a bias toward higher or lower magnitude estimates.

7. The use of vertical-component seismometers instead of the original Wood-Anderson horizontal torsion seismometers used by Richter may affect the magnitude estimate to a degree.

Of the above biases, 2, 4, 6 and 7 are ignored in the everyday earthquake magnitude estimation process. The magnitude is determined for each seismogram and the mean is reported as the local magnitude, M_L . This estimate is probably accurate to within half a magnitude unit.

Since one of the objectives of this study is to define the Benioff zone in central Alaska, knowledge about the accuracy of the focal depth for each earthquake is extremely important. Earlier workers (VanWormer et al., 1974, and Davies, 1975) had difficulty in fixing the depths of earthquake foci in central Alaska. The first computer program used by the Geophysical Institute, EPICNTR, had no provision to detect the failure of input data to fix focal depths, and it only gave discrete depths derived from the Herrin tables (1968). Using EPICNTR, Davies (1975) found that, on the average, Geophysical Institute focal estimates tended to be about 28 km deeper than those of NOAA.

The computer program of Lee and Lahr (1971, 1975), called HYP071, attempts to solve the depth control problem by using an iterative method. If the travel-time errors begin to increase, the depth is fixed until the epicenter is relocated well enough to allow continued trial depth variation to achieve a best fit. HYP071 also allows the inclusion of S-wave first motion data which, in principle, should make the final solutions even more accurate. However, it is usually very hard to read

the onset of the S-wave to within a tenth of a second. Most of the earthquakes of Group III did not have readable S-arrivals.

The earthquakes of Group III which had listed S-arrivals were reread and run on HYP071 using both the P- and S-arrival times in an attempt to compare the depths to those when only the P-arrival was used. Table 5 shows the results.

In general, the residuals increased when both P and S were used, probably due to the fact that S is so hard to read on the film records used. Those four earthquakes that displayed decreasing residuals yielded only slightly better residuals and moderately deeper foci.

For the earthquakes that had only three or four readable station records, it appears that better depths are obtained using both P and S, as long as the residuals are small. The depth to focus using only the P-arrival is satisfactory compared to the depth using both P and S, provided that the difference in residuals is small. Thus it appears that satisfactory depth control is achieved using only the P-arrival.

It is useful to have the S-arrival listed on scaling sheets when it can be read. An additional S-arrival reading can act as an "extra station" for those earthquakes having only three or four readable P-arrivals, and can act as a check on the depths of all events when only P-arrivals are used.

Table 6 permits a comparison of the average depth of earthquakes obtained using HYP071 on Geophysical Institute data to those of NOAA. The standard deviation of the difference in focal depth has dropped steadily over the four-year period, indicating that the two groups have more compatible depths later in the catalog.

4. PRESENTATION OF DATA

4.1 General Seismicity

The proportion of large earthquakes to small earthquakes for any area can be estimated using the Gutenberg-Richter formula:

$$\log_{10} N(M) = a - b M \quad (3)$$

in which $N(M)$ is the number of earthquakes with magnitude equal to or greater than M , and a and b are constants which take on certain values depending upon location and epoch. The constant a is the base-10 logarithm of the number of events with magnitudes greater than zero. The value of b is a significant parameter describing the distribution of earthquakes by magnitude (Gutenberg and Richter, 1944; Richter, 1958). The value of b ranges from 0.6 to 1.2 for different areas (Lee and Stewart, 1980). The worldwide average for b is approximately 0.9 (Utsu, 1969) to 1.0 (Rikitake, 1976), so that the frequency of earthquakes at magnitude $(M-1)$ is approximately eight to ten times greater than at M .

To find a b -slope for an area one can make a cumulative plot of $\log N(M)$ vs. M . Ryall et al. (1968) recommend magnitude intervals of 0.1 for best results. A deviation from linearity will occur at the lower magnitudes and possibly at the extreme upper magnitudes. The deviation at the lower magnitudes is generally ascribed to the incomplete detection of small-magnitude earthquakes. A cutoff magnitude, M_0 , must be chosen above the beginning of

curvature; M_0 is usually chosen quite close to the minimum size of earthquakes that can be uniformly detected by the recording network (Savage, 1976). It defines the magnitude above which the earthquake data set can be considered statistically complete. For a determination of b-slope, a uniform data set is necessary.

Utsu (1965) and Lomnitz (1966) have specified the calculation of b as:

$$b = \frac{0.4343}{\bar{M}(M_0) - M_0} \quad (4)$$

where $\bar{M}(M_0)$ is the mean magnitude of all events with magnitude equal to or greater than the cutoff magnitude, M_0 . Aki (1965) demonstrates that this is the maximum likelihood estimator of b. The method of maximum likelihood is the most accurate way of determining b-slope (Savage, 1976; Knopoff and Kagan, 1977) but it has large error estimates, especially for low b-slopes (Savage, 1976).

The error estimates for the maximum likelihood technique are given, for the 95% confidence level, by Aki (1965) as:

$$\frac{1 - 1.96\sqrt{n}}{\bar{M}(M_0) - M_0} \leq b' \leq \frac{1 + 1.96\sqrt{n}}{\bar{M}(M_0) - M_0} \quad (5)$$

where $b' = b \ln 10$ and n is the number of earthquakes used. The confidence limits give a measure of the random data variation and not the quality of linear fit (Savage, 1976).

For comparison of significant differences in b-slope between two sets of data, Cox and Lewis (1966) give confidence limits as:

$$\frac{b_1 - b_2}{\frac{b_1^2 [\ln 10]}{n_1} + \frac{b_2^2 [\ln 10]}{n_2}} \leq t_{c1, n-1} \quad (6)$$

where b_1 is larger than b_2 , and t_{c1} is the t-test number for a given confidence level for $n-1$ degrees of freedom. This method has been applied to the study of foreshock and aftershock sequences of large earthquakes with good results. Precursory drops in b have been reported prior to large events with a subsequent return to normal or above-normal b -slope during the aftershock sequence (VanWormer et al., 1975; Bufe, 1970; Wyss and Lee, 1973; Bolt, Stifter and Uhrhammer, 1977). For these types of comparisons, Savage (1976) recommends sample sizes of 100 b and magnitude ranges of at least two units for best results, since the confidence limits for small samples are so large that b -slope comparison is almost meaningless.

Bufe (1970) used a sliding event-window of 50 earthquakes to observe temporal changes in b near Danville, California, and found large variations in b (from 0.6 to 1.17) with the extreme values occurring near the times of large earthquakes. There are few explanations why the value of b changes with time. From laboratory experiments on rock fracture, Scholz (1968) found an inverse relationship between applied compressive stress and b -slope. He

attributed high values of b to crack closure and frictional sliding, while low b occurred during propagation of new fractures. Thus it seems that for certain earthquake-prone areas, a statistically significant low value of b may be an indicator of high stress buildup, to be followed by a large earthquake.

Results of this application of b -slope to the study area are as shown by Figures 7 and 8. These curves represent cumulative plots of $\text{Log } N(M)$ vs M for earthquakes in Groups II and III, respectively. The cutoff magnitude, M_0 , is 2.8 for both groups, i.e., the data set for this study is complete above magnitude 2.8. Using a modified form of a computer program described by Huang (1979), the b -slope and confidence interval for 2,037 earthquakes of magnitude 2.8 or greater from October, 1967 to December, 1978 was found to be 1.00 ± 0.04 at the 95% confidence level. A search for foreshocks and aftershocks of the largest events ($M_L > 5.0$) in the area yielded very few earthquakes. Therefore, no comparisons of b -slope for statistically significant precursory changes can be made with the present data set. However, a sliding 200-event window for groups II and III produces very large changes in b -slope over time (Table 7), similar to those reported by Bufe (1970). The smallest b -values are associated with the larger ($M_L > 5.0$) earthquakes.

The value of a in the Gutenberg-Richter formula was found empirically as follows. There were 149 earthquakes in the 11.3-year epoch September 1967 to December 1978 which had magnitudes

greater than or equal to 4.0. Setting $M = 4.0$ in the equation $\log N(M) = a - 1.0 M$, yields $a = 6.17$. To facilitate comparisons of seismicity levels between this area and other parts of Alaska, the value of a was also determined in units of $\text{year}^{-1} \text{degree}^{-2}$, where one square degree is equivalent to a block 110 km on a side. For the ten-square-degree study area,

$$a = \log \frac{10^{6.17}}{(10 \text{ degree}^2)(11.3 \text{ yr})} = 4.1 \text{ yr}^{-1} \text{degree}^{-2} \quad (7)$$

This level of seismicity is over twice as high as that found for the Fairbanks area ($a = 3.69 \text{ yr}^{-1} \text{degree}^{-2}$) and over 19 times as high as an area to the east ($a = 2.82 \text{ yr}^{-1} \text{degree}^{-2}$) (see Davis, 1978).

4.2 Energy Release and Number of Events per Month

The amount of energy E , in ergs, released by an earthquake is related to its local magnitude (M_L) by the equation (Richter, 1958):

$$\log E = 9.9 + 1.9M_L - 0.024 M_L^2 \quad (8)$$

Figures 9 and 10 show the number of earthquakes per month and the energy release per month using data from Groups II and III for the epoch September 1967 to December 1978.

The low number of earthquakes in the latter half of 1976 (Figure 9) is due in part to a lack of satisfactory record-reading;

only the largest events were located. However, scaling of two months of data by the author indicates that the micro-seismicity level for July and August 1976 is lower than normal for the rest of the year. Still, the energy release for the same period is not anomalously low since the number of earthquakes with magnitudes greater than 4.0 is not significantly different than before or after this period.

Note that in Figure 9 the numbers of earthquakes during April and May 1972 are more than three standard deviations above the mean number of earthquakes per month. This anomaly is statistically significant at the 95% confidence level (F-test). Earthquakes both above and below the cutoff magnitude of 2.8 account for the increase. High seismicity continued until August 1972. In September, only six earthquakes above magnitude 2.8 occurred, but microseismicity (here considered as those earthquakes with magnitudes less than 2.8) increased. A magnitude 5.2 earthquake occurred on October 1, whereupon the magnitude distribution of seismicity during succeeding months returned to normal. No other sequence of this type occurs in the data, so it is not known if this type of precursory activity is significant. Because of the great variability in station coverage, the data cannot be tested statistically for recurrence cycles.

4.3 The Benioff Zone

Previous authors (VanWormer et al., 1974; Davies, 1975) have

concluded that the dipping earthquake zone in Alaska trends N17°E through Cook Inlet to the Yenta River Region, where it bends 30 degrees to the east, striking N47°E to within 75 km of Fairbanks.

This study includes all earthquakes from the Yentna River north to the northern foothills of the Alaskan Range. Group III earthquakes (epoch May 1974 to December 1978) were projected onto vertical planes using a computer program (Davies, 1975), to better define the strike direction in this area. Figure 11 shows a view of all Group III events looking N17°E. The Benioff zone can be seen but appears very diffuse, extending to about 150 km depth. Estes (1978) has written a computer program which fits a least-squares plane to all earthquakes between specified depths. Using Estes' program for all events between 50 km and 150 km, the best-fit strike of the Benioff zone is approximately N44°E, with a standard deviation of the hypocenter distances from the dipping plane of 17.6 km. Figure 12 shows a view looking northeast along this best-fit strike. The Benioff zone seems to be more clearly defined at this direction of strike than at N17°E. The thickness of the zone is 25 to 30 km, as defined by the majority of the earthquakes.

Those earthquakes below approximately 175 km may be poorly located since they do not obviously correspond to the Benioff zone. The concentrations of hypocenters at depths of zero, 5 and 33 km in Figures 11 and 12 are due in part to the fact that the computer program used to locate the earthquakes, HYP071, tends to constrain depths to zero or 5 km if there are not enough station records or

if the scaled times are poor. Many of the earthquakes in the NOAA catalog are constrained to 33 km depth for similar reasons. Therefore, the concentrations of activity at these depths should not be taken at face value as indicative of true crustal earthquake activity.

As can be seen in Figure 12, the Pacific plate dips at a small angle of 15 to 20 degrees as it is forced under southern Alaska, then dips at 45 to 50 degrees under the southeast flank of the Alaska Range to a depth of 150 km near Mt. McKinley. A vertical plane view at 90 degrees to the strike shows the lateral extent of earthquake activity along the subduction zone (Figure 13). The area of highest earthquake activity lies beneath Mt. McKinley at depths of 100 to 150 km. The Yentna River area, to the southwest of Mt. McKinley, has very few events below 100 km. Thus, application of the Group III data set produces similar results to that obtained by Davies (1975) who postulated that the change in strike in the Yentna area was a structural break in the subducting plate. To the northeast, the number of earthquakes at depths between 100 to 150 km drops off near a cluster of events located at 64.1°N, 148.0°W, suggesting that this may be the northeastern extent of Pacific plate subduction in Alaska.

Other papers on subduction zone seismicity (Barazangi and Isacks, 1979, for example) have shown that the Benioff zone may be more accurately determined using only the best-located events which pass certain quality constraints. Pursuing this idea, six con-

straints were placed on the data from Group III as follows:

1.	RMS \leq 1.0 sec	88.9% pass
2.	ERH \leq 10.0 km	75.2% pass
3.	ERZ \leq 10.0 km	58.9% pass
4.	GAP \leq 160.0 degrees	28.2% pass
5.	number of stations \geq 5	55.7% pass
6.	DMIN/DEPTH ratio \leq 100	96.4% pass

Approximately 13.7% of the earthquakes passed all six constraints, amounting to 353 events.

To better define the northern end of plate subduction, the data set was expanded to include an adjacent area to the northeast. The additional area is bounded by 64.05° to 64.5° North latitude, 145.8° to 150.0° West longitude. This increase in the size of the area resulted in the addition of 65 earthquakes from the same epoch which passed all 6 constraints. A map view of these 418 earthquakes appears in Figure 14. The letters there stand for focal depth: A is 0 - 25 km, B is 25 - 50 km, etc. The sizes of the letters are proportional to the magnitude of the earthquakes; latitude and longitude numbers are approximately equal to the size of a magnitude 2.0 earthquake. The earthquakes are located at the lower left corner of each letter.

Using Estes' (1978) computer program, the best least-squares fit for all constrained earthquakes between 50 and 150 km. depth (190 total events) is a plane striking $N52^\circ E$ (Figures 15, 16), with

a standard deviation of the hypocenter distances from the dipping plane of 12 km. This strike is 8 degrees more easterly than the strike of $N44^{\circ}E$ obtained by using all the earthquakes of Group III.

The large azimuthal difference in strike may be due to the small number of earthquakes between 50 and 150 km depth which passed the constraints. Another possibility for the azimuthal difference may be that the dipping plate does not have a linear strike as it descends beneath the Alaska Range. Thus, a change in the proportion of events along different parts of the Benioff zone could account for the large variation in strike azimuth as obtained by a least-squares fit. A comparison of Figure 16 with Figure 13 shows that for all the earthquakes, a greater proportion of events in Figure 13 are located under the Mt. McKinley region, whereas the locations of the constrained earthquakes are more evenly spaced along the strike. Figure 17 shows two stereoscopic pairs of the best-fit (constrained) earthquakes. The top stereoscopic pair shows a view approximately along the strike looking northeast, and the bottom view is 90 degrees to it, looking northwest. One can see in the top stereoscopic pair that the strike is not linear, but bends slightly to the north at the northeast end.

The northeastern end of the Benioff zone, as seen from the constrained events in Figure 16, is located at approximately $64.1^{\circ}N$, $148.0^{\circ}W$, the same as before when all the earthquakes were used.

In Figure 16, no constrained events are located below 85 km depth near the Yentna lineament. There is a abrupt appearance of earthquakes at intermediate depths to the northeast, beginning under Mt. McKinley. It appears that the anomaly or structural break in the Yentna region, proposed by VanWormer et al. (1974) and Davies (1975), is real.

A map view of the 75-, 100-, and 125-km depth contours of the Pacific plate Benioff zone is shown in Figure 18. Subduction clearly extends approximately 45 km north of the Hines Creek strand of the Denali Fault, ending at depth in the northern foothills of the Alaska Range. The 75-km depth contour is dashed due to the small number of earthquakes used in its location. The 150-km depth contour is not shown since no well-located events occurred at or below this depth. The deepest well-located earthquake had a focus at 148 km depth.

4.4 Strain Release

For purposes of energy calculation, Gutenberg and Richter (Richter, 1958) recommend using a "unified magnitude scale" in which all magnitude estimates are reduced to the teleseismic body wave magnitude (m). The relation between energy release and magnitude of an earthquake can be expressed by the equation (Bath, 1973):

$$\log E = 4.78 + 2.57 m \quad (9)$$

where m is the body-wave magnitude empirically related to the Richter magnitude, M_L , by $m = 1.7 + 0.8 M_L - 0.01 M_L^2$, and E is in ergs.

Strain release is proportional to the square root of energy (Richter, 1958). Since a summation of strain release for many earthquakes produces very large numbers, the log of strain release is usually used for contour maps, and that convention is adopted here.

Strain release maps have been compiled using all earthquakes from Groups II and III (epoch September 1967 to December 1978). The study area was divided into 20-km square blocks and the strain release for each block was summed for all events in the block. Each earthquake was assumed to be a point source of energy. Since the earthquake locations are generally accurate to within 20 km for the larger events, the block method appears adequate for a preliminary contour map. The largest earthquake in the area during this time period, magnitude 5.6, was located at 62.0°N, 151.2°W. It occurred November 3, 1970, at 70 km depth (NOAA solution). Since Anderson (1979) has shown that most estimates of fault rupture length for an earthquake of this magnitude fall well below 20 km, the error involved in assuming the earthquakes to be point sources probably is low.

A modified version of a computer program prepared by Estes (personal communication) was used to sum the strain release for all blocks, and the resulting numbers were hand-contoured. The maps

appear in Figures 19, 20, and 21. Figure 19 represents the strain release for all earthquakes with hypocenters of 30 km or less, and Figure 20 represents strain release for all hypocenters of more than 30 km depth. Figure 21 represents strain release summed for all hypocenters regardless of depth. Faults (from Beikman, 1974) and the 75-, 100- and 125-km depth contours of the Benioff zone are shown superimposed on all three maps, along with the location of the Alaska Railroad (ARR). A contour of numerical value 10 corresponds to the summed equivalent of one magnitude 5.7 earthquake per block. Most of the strain release is associated with the subduction zone (Figures 19, 20), especially at its northeastern and southwestern ends. In general, the northeast end of the subduction zone has exhibited strain release at shallow depths while the strain at the southwestern end has been relieved at depths over 30 km. Note that the total amount of strain release (Figure 21) drops off to the southwest of Mt. McKinley in the vicinity of the Yentna River; only small-magnitude earthquakes have occurred there since 1967, although larger events may have occurred in the Yentna area in the past (see Table 1).

One area in the upper Susitna River valley shows what may be an anomalously low amount of strain release, indicating a possible strain accumulation there (Figure 21). It appears to be surrounded by areas of larger strain release. An earthquake of magnitude 5.2 would effectively fill this gap, so the low area is probably not significant.

Some strain release does seem to be associated with the McKinley strand of the Denali Fault (Figure 19) at approximately 63.5°N, 147.5°W, and also with the Farewell segment at approximately 62.6°N, 152.8°W. When the strain release is summed for both shallow and intermediate depth (over 30 km) earthquakes, there does appear to be some strain release along the Iditarod-Nixon Fork Fault (Figure 21). The Susitna fault also exhibits moderate strain release at its northeastern and southwestern ends (Figure 21).

5. DISCUSSION

The chief result of this study is the delineation of the Benioff zone in the central Alaska Range north of 62° North latitude and the location of its northeastern extent at approximately 64.1°N, 148.0°W.

The strike of the Benioff zone near its northern end is N44°E if all earthquake data are used, without regard to quality of epicenter locations. When only the best-located earthquakes are used, the strike is N52°E. The strike using only the constrained data is the more reliable of the two, and is only slightly different from the strike of N47°E found by Davies (1975). The difference is most likely due to the increase in station coverage and the more sophisticated location program and velocity model employed subsequent to Davies' study. The low number of intermediate-depth earthquakes in the Yentna area from September 1974 to December 1978 (Figures 13, 16) and the low amount of strain release there (Figure 21) is in agreement with Davies' hypothesis (1975) that the eastern part of the Aleutian-Alaskan Benioff zone is split into

several distinct blocks. From this study the McKinley Block (Davies, 1975) appears to be separate from the Kenai Block along the Yentna lineament. However, it is possible that the subducting slab exists in the Yentna area but has not yet reached intermediate depths. One other possibility may be that the subduction process occurs aseismically at intermediate depths in this region.

Since most of the seismometer stations are located around the eastern part of the study area (Figure 3), the earthquake waves traveling up the high-velocity subducting slab will reach a major proportion of the stations earlier than predicted by the horizontal-layer velocity model (Table 3). This earlier arrival may tend to pull the computed intermediate depth earthquake locations, in the lower part of the subducting slab, toward the east. The sudden change in dip of the Benioff zone at about the 90 km depth interval (Figures 12 and 15) could be an actual structural feature of the slab, but it is more likely due to the present velocity model used to obtain earthquake locations. In a study of central Aleutian earthquakes, Engdahl (1973) showed that a three-dimensional velocity model effectively straightens the abrupt change in dip originally found into a more continuously curving plunge. Relocating the McKinley block earthquakes with a three-dimensional velocity model probably would show the true dip of the Benioff zone.

One of the most interesting features of the subduction zone under Mt. McKinley and to the northeast is the almost total lack of volcanic activity. Subduction extends to a depth of 150 km along this part of the Benioff zone. To the southwest, outside the study area, many

volcanoes are situated above the 100-km depth interval. Plafker (1969), Davies and Berg (1973) and Davies and House (1979) suggest that the lack of volcanoes to the northeast is due to the great distance that the Pacific plate travels under southern Alaska at a shallow-angle dip, extending 300 km from the trench before plunging at a steeper angle more typical of other subduction zones. They suggest that the trench sediments and water are scraped off before the 100-km depth interval is reached, where they would normally take part in the production of andesitic magmas, forming volcanoes at the surface. In a recent study, Albanese (1980) reports a Recent pair of small, maar-like features near the northeastern end of Pacific plate subduction at $64^{\circ}3.5'N$, $148^{\circ}25'W$, which she has dated at 3,000 years \pm 1,000 years using the C14 method on burnt humus layers beneath the cinder blanket. She also reports that the tholeiitic basalt cinders from these explosion features have striking similarities to Aleutian basalts, and are derived from a relatively primitive, undifferentiated source at considerable depth in the upper mantle. This seems to support the arguments of Plafker (1969), Davies and Berg (1973) and Davies and House (1979). No andesitic magmas are produced due to a lack of sediments and sufficient water at depths conducive to their partial melting, below 60 to 80 km (Schwarz et al., 1977). If partially dehydrated material of the Pacific oceanic crust is subducted to intermediate depths, small amounts of basaltic magma may be produced by mixing of partial melt from the subducted plate with the overlying mantle (Ringwood, 1974; Kay, 1977). Davies (1975) found marginal seismic evidence for partial melting at the 115-km depth

interval in the Benioff zone under the Mt. McKinley region. Perhaps basaltic volcanic activity over this part of the subduction zone is just beginning.

Referring to Figure 18, the trace of the Denali Fault east of 147° West longitude appears to closely parallel the direction of Pacific plate subduction. Movement of this part of the fault is dextral strike-slip; the fault has been described as a transform fault (Tobin and Sykes, 1968). West of 150° W, the Denali Fault trace is approximately normal to the subduction direction and a large proportion of offset on this part of the fault is vertical with the south side moving relatively upward (Grantz, 1966). Between 147° W to 150° W along the McKinley strand, both strike-slip and vertical movements have been found (Reed and Lanphere, 1974). The marked increase of vertical offset from east to west along the fault is easily explained. Compressive stresses created by the subducting plate have paralleled the eastern part of the Denali Fault causing dextral strike-slip movement there, while the stresses have been more nearly perpendicular to the Farewell Fault segment, causing vertical thrusting on it. The McKinley and Hines Creek strands appear to be part of a transition zone along the fault trace between strike-slip and vertical movements. This part of the Denali Fault rounds off the northeast corner of the subducting plate, at least as a surficial feature. The Hines Creek strand is older than the McKinley strand and may not have undergone offset attributable to the present subduction of the Pacific plate (Lanphere, 1978), but the McKinley strand has undergone Recent movement (Grantz, 1966). Several

of the shallow best-located earthquakes appear to fall on or near the McKinley strand (Figure 18) but no fieldwork has been done to check for offset due to these small shocks.

The Army Corps of Engineers has proposed the construction of two hydroelectric dams on the Susitna River. Both sites lie within the area examined in this thesis. The Watana Dam site is located at approximately 62.83°N , 148.5°W , and the Devil Canyon site is farther downriver at approximately 62.83°N , 149.34°W .

Figure 22 contains a map view of all earthquakes of magnitude 3.5 or greater occurring from August 27, 1904 to August 31, 1967 within the boundaries shown. The Devil Canyon (DC) and Watana (W) dam sites are shown with concentric circles of radii 25 and 50 km. An earthquake of magnitude 6.25 on July 3, 1929 was given an epicenter location within 50 km of both dam sites. On May 2, 1963 a magnitude 5.1 earthquake occurred within 50 km of the Devil Canyon site. Also, two earthquakes of magnitude 5.6 and 5.1 have been located within 25 km of the Devil Canyon site, on May 29, 1931 and December 14, 1963, respectively. Figure 23 shows the same area with all earthquakes of magnitude 3.5 or greater for the epoch September 1967 to April 1974. A magnitude 5.2 earthquake on October 1, 1972 has been located within 25 km of the Devil Canyon site and also within 50 km of the Watana site. An earthquake of magnitude 4.5 occurred within 25 km of the Watana dam site on December 28, 1968. On February 5, 1974 a magnitude 4.7 earthquake occurred within 50 km of both sites.

Figure 24 shows the same area with all earthquakes of magnitude 3.5 or greater for the epoch May 1974 to December 1978. A magnitude-5.2 earthquake was located approximately 62 km northwest of the Devil Canyon site on May 18, 1975. Three earthquakes of magnitude 4.6, 4.5 and 4.25 have been located within 25 km of the Devil Canyon site, and two events of magnitude 4.8 and 4.6 occurred within 50 km of the Watana site during this time period. A magnitude-4.46 earthquake was given an epicenter within 50 km of both sites on April 2, 1978.

Figure 25 gives the relative Richter magnitudes for the letters representing earthquakes on Figures 22, 23 and 24. The earthquakes are located at the lower left corner of each letter. An A stands for a hypocentral depth of 0-25 km; B is 25-50 km, etc. Table 8 gives all earthquakes occurring within approximately 50 km of either dam site.

From the data presented, it appears that no major earthquakes ($M \geq 7.0$) have occurred in the immediate vicinity of the two proposed dam sites since records have been kept. However, two major earthquakes may have occurred within 180 km of the sites since 1904. The first earthquake of major size was the August 27, 1904 ($M = 7\text{-}3/4$ to $8\text{-}1/4$) event which has been given a nearest-degree location of 64°N , 151°W (Figure 22), but this earthquake is poorly located (see section 2). On July 7, 1912 California seismographs registered a magnitude 7.4 earthquake which was assigned the location 64°N , 147°W (Figure 22). The location accuracy of this event is unknown. A third major or "great" earthquake was the accurately-located event of March 28, 1964, in Prince William Sound with a magnitude estimated between 8.3 to 8.6 (Plafker,

1969). The epicenter of this event is approximately 220 km from the dam sites.

Kelleher et al. (1974) conclude that, for Pacific subduction zones, there is a strong positive correlation between the length of shallow, low-angle thrusting of the downgoing slab and maximum observed earthquake magnitudes. The greatest depth of low-angle thrusting varies among island arcs but does not generally exceed 60 to 70 km (Isacks and Molnar, 1971). More recent investigations of Aleutian-Alaskan seismicity place the maximum depth of the shallow main thrust zone at 40 km (Jacob et al., 1977; Pulpan and Kienle, 1979; Davies and House, 1979). Rupture zones of the major earthquakes seem to be confined to the shallow thrust zone. This shallow thrust zone widens from west to east along the Aleutian-Alaskan arc, reaching an unusually large width near the epicenter of the 1964 earthquake (Lahr and Page, 1972). The shallow-dipping interface between the subducting Pacific plate and the Alaskan continental crust extends from the eastern Aleutian trench under Prince William Sound to near the Talkeetna Mountains. The subducting plate continues under the Susitna dam sites and begins a steeper descent at approximately the 90 km depth level (Figure 15).

The Devil Canyon dam site lies approximately over the 65-km depth contour of the upper surface of the Benioff zone based on the best-located earthquakes from May 1974 to December 1978. The seismicity under the Watana site for the same period is more diffuse, but the interface between Alaskan continental crust and Pacific plate probably lies between 55 to 65 km below the site. In view of the works cited

above, the Benioff zone directly under the dam sites is probably not capable of a major earthquake. The historical seismicity around the sites seems to support this hypothesis. The aftershock zone of the 1964 Prince William Sound earthquake did not extend as far north as the dam sites (Sykes, 1971).

6. CONCLUSIONS

The following conclusions are drawn from this study:

1. The Benioff zone extends from the Cook Inlet region under the central Alaska Range with a direction of strike approximately N52°E. The northeastern limit to the subduction zone is located at 64.1°N, 148°W, in the northern foothills of the Alaska Range. Results show that the Pacific plate is probably thrusting under the Alaskan continental block from the southeast at a shallow angle of 15° to 20° until the 90-km depth level is reached. Below 90 km the plate dips more steeply at 45° to 50° to a depth of 150 km; the abruptness of the change in dip at the 90-km level may be a result of the velocity model used. The Yentna River section of the Benioff zone, to the southwest of Mt. McKinley, appears to be anomalous in its lack of intermediate-depth earthquakes.
2. The level of seismicity in the study area is approximately twice as high as in the Fairbanks region and is described by the relation $\log N(M) = 4.1 - 1.0M$, where $N(M)$ is the number of earthquakes with magnitudes equal to or greater than M each

year in an area one latitude-degree square. Most of the strain release in the area is associated with the subduction zone. There is some evidence for fault-related strain release, but this interpretation is tentative and based on few well-located earthquakes.

3. Evidence from felt reports indicates that the $M = 7\text{-}3/4$ to $8\text{-}1/4$ earthquake of August 27, 1904 may be poorly located and perhaps is located to the west of the study area.
4. The subducting Pacific plate lies at a depth of 55- to 65-km beneath the proposed Susitna dam sites. Very large earthquakes probably will not occur along this section of the submerging plate, but the sites do lie to the northwest of an area known to undergo major earthquakes associated with the shallow thrust zone.

Suggestions for Future Seismic Work

1. The anomalous Yentna River area should be investigated with portable or permanent seismometer stations to determine if the lack of intermediate-depth seismicity is real or merely a result of the present station locations.
2. A three-dimensional velocity model similar to that of Engdahl (1973) should be applied to a relocation of the earthquakes in the study area to determine if the abrupt change in dip of the Benioff zone at depth 90 km is real.

3. One might be able to predict the occurrence of potentially destructive earthquakes in this area with a continuing program that includes continuous updating of the strain-release maps and b-slopes.
4. To help in siting future seismometer stations, a contour map of RMS travel time errors should be made to show areal trends in the errors.
5. To better define the depth to focus and reduce GAP to a minimum, several seismometers should be placed on the northwest flank of the Denali-Farewell fault region of the Alaska Range. One site with relatively easy summer access is the Kantishna area.
6. The data from Group II, epoch October 1967 to April 1974, should be relocated using the computer program HYP071 (Lee and Lahr, 1971, 1975).

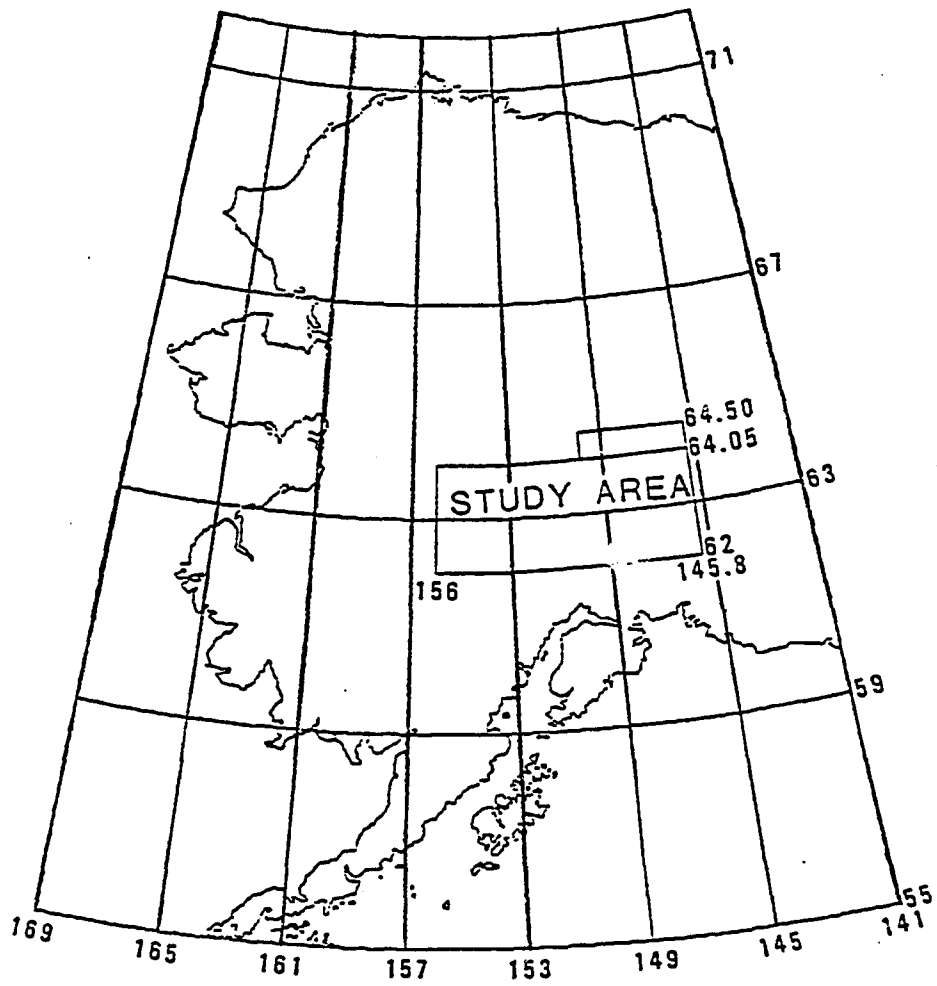


Figure 1 - The boundaries of the area studied in this thesis. The small area to the northeast was added to better define the end of the Benioff zone.

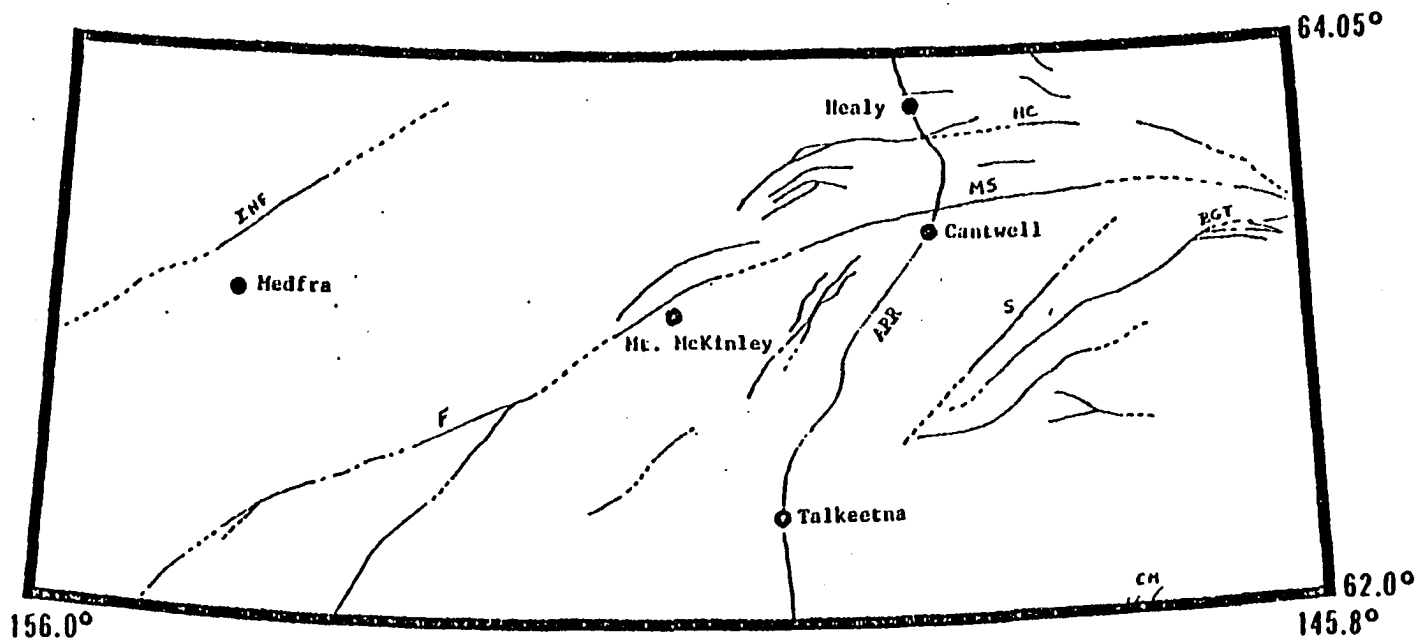


Figure 2 - Known faults within the study area (taken from Beikman, 1974). Named faults include the Iditarod-Nixon Fork fault (INF), Hines Creek Strand (HC), McKinley Strand (MS), Farewell fault (F), Susitna fault (S), Broxson Gulch Thrust fault (BGT), and the Castle Mountain fault (CM). ARR - Alaska Railroad.

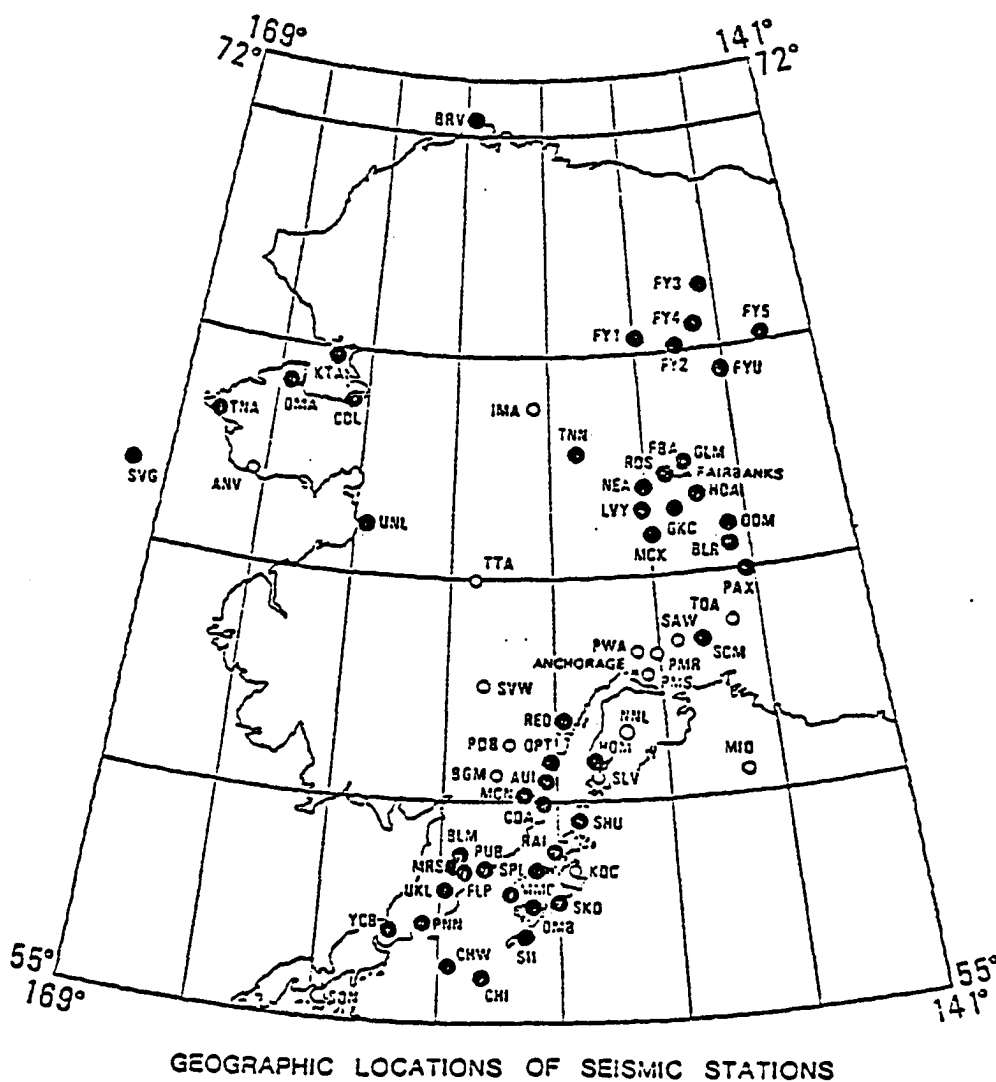


Figure 3 - Present location of seismometer stations. The closed circles (●) indicate Geophysical Institute stations; open circles indicate NOAA stations.

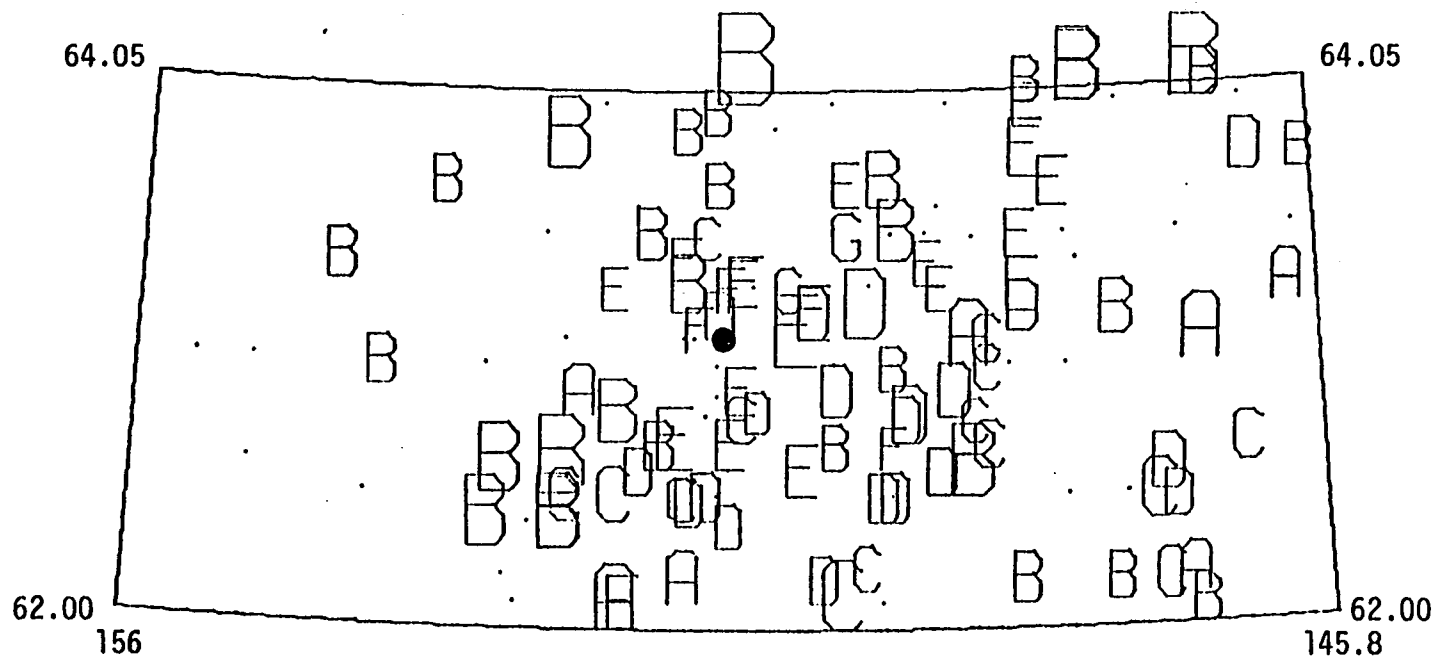


Figure 4 - All earthquakes in the study area from August 1904 to August 1967. The earthquakes are located at the lower left corner of each letter. Letters stand for focal depth; A = 0-25 km, B - 25-50 km, etc. The size of the letter indicates the magnitude of the earthquake as shown in Figure 25. Dots represent earthquakes having unknown magnitude. The circle (●) indicates the location of Mt. McKinley.

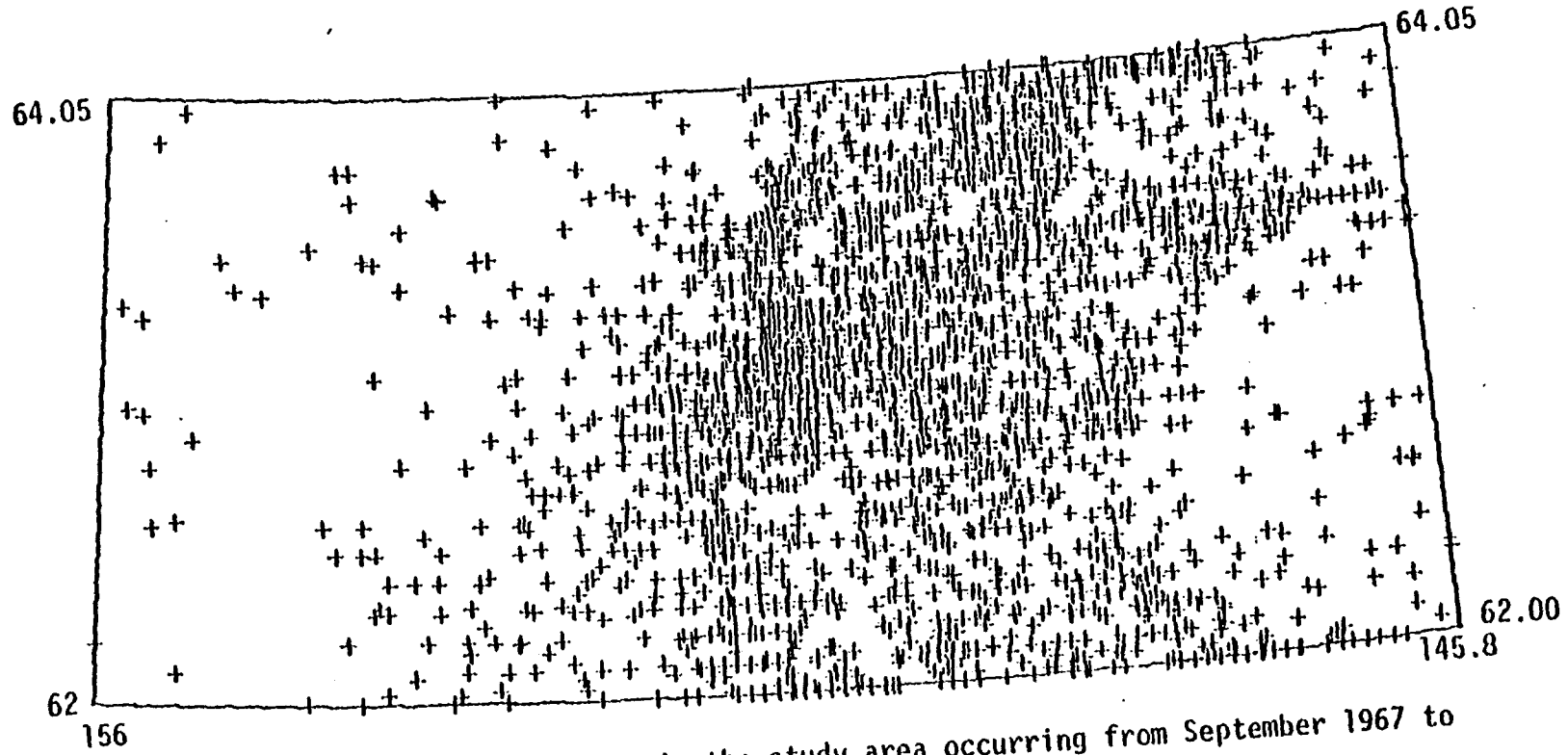


Figure 5 - All located earthquakes in the study area occurring from September 1967 to April 1974.

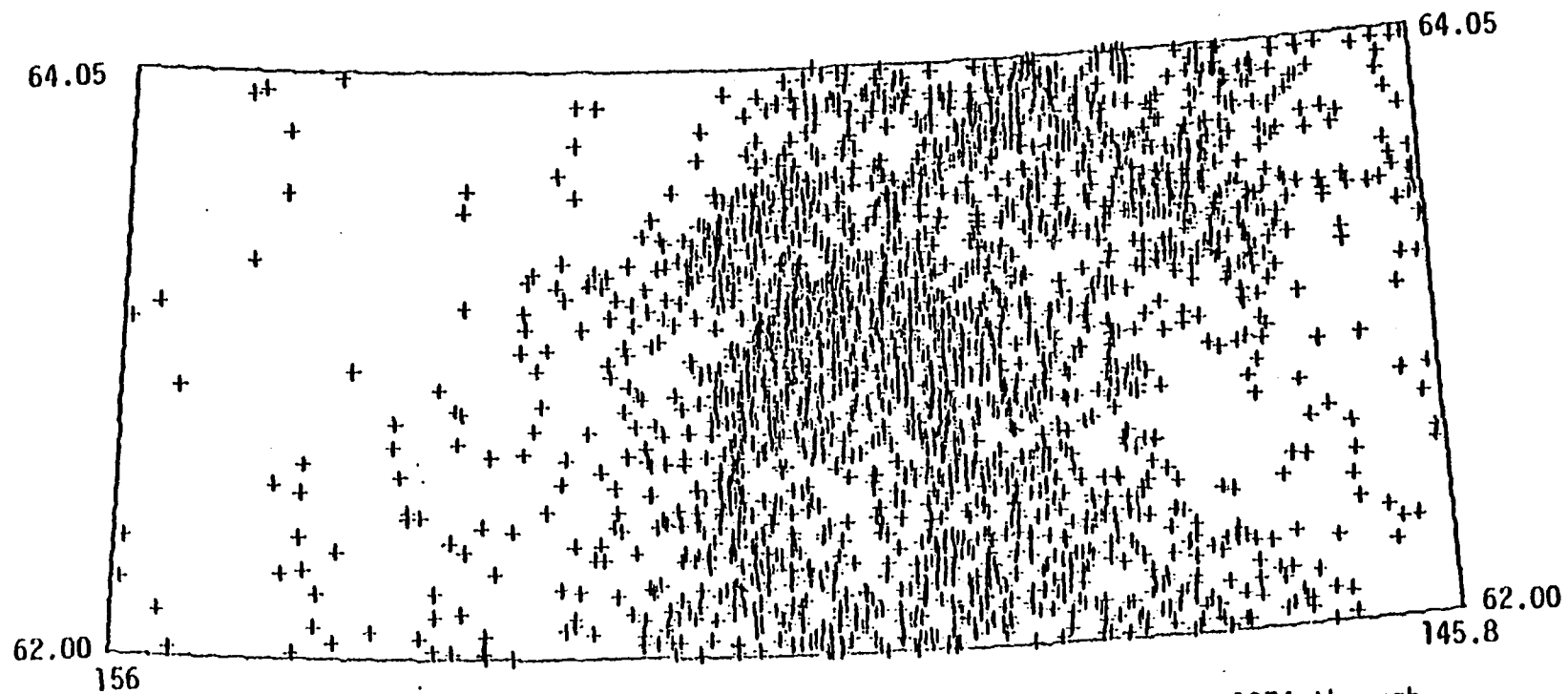


Figure 6 - All located earthquakes in the study area occurring from May 1974 through December 1978.

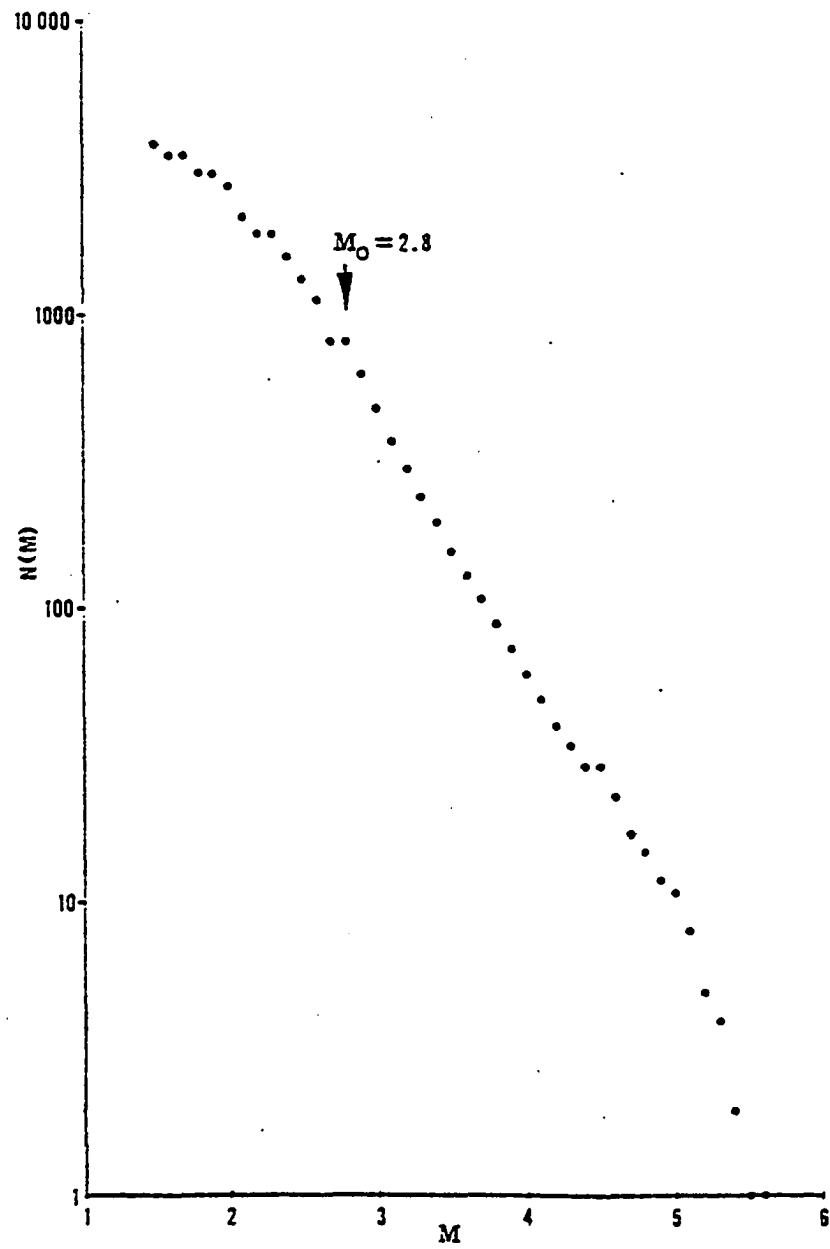


Fig. 7 - Cumulative magnitude plot of all earthquakes from Sept. 1967 to April 1974. Cutoff magnitude $M_0 = 2.8$.



Fig. 8 - Cumulative magnitude plot of all earthquakes from May 1974 to Dec. 1978. Cutoff magnitude $M_0 = 2.8$.

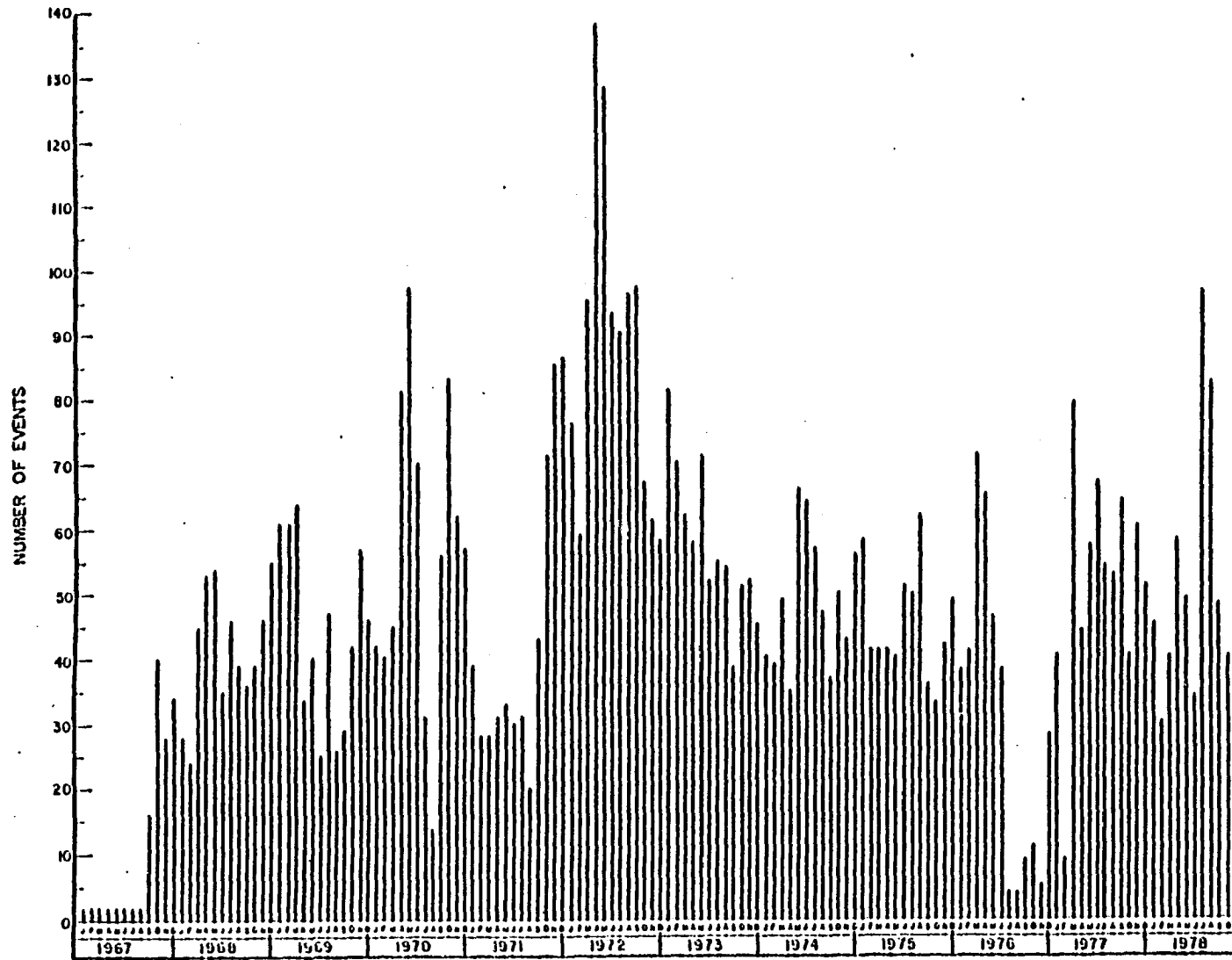


Figure 9 - Number of earthquakes per month from September 1967 through December 1978.

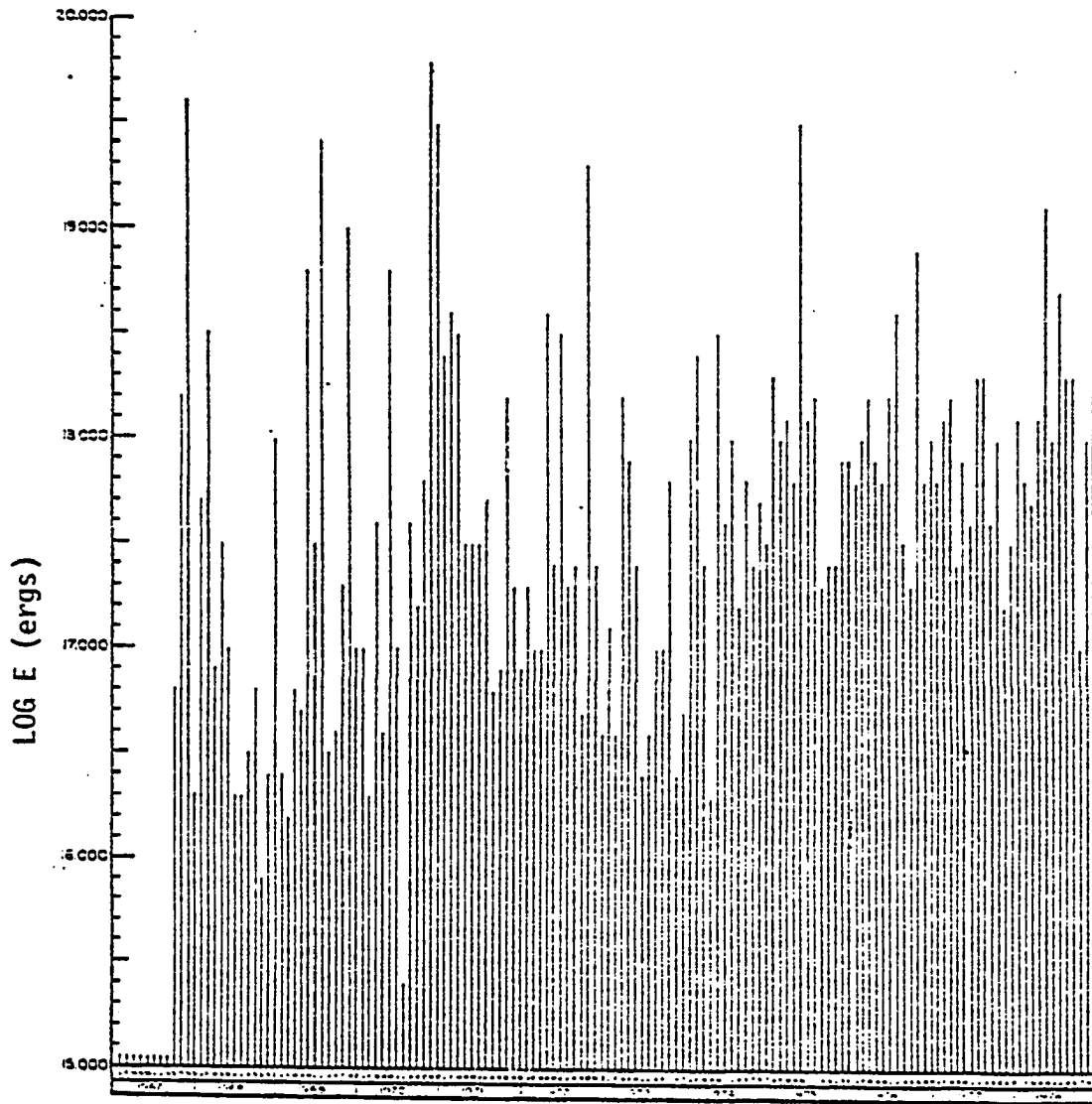


Figure 10 - Energy release per month from September 1967 through December 1978.

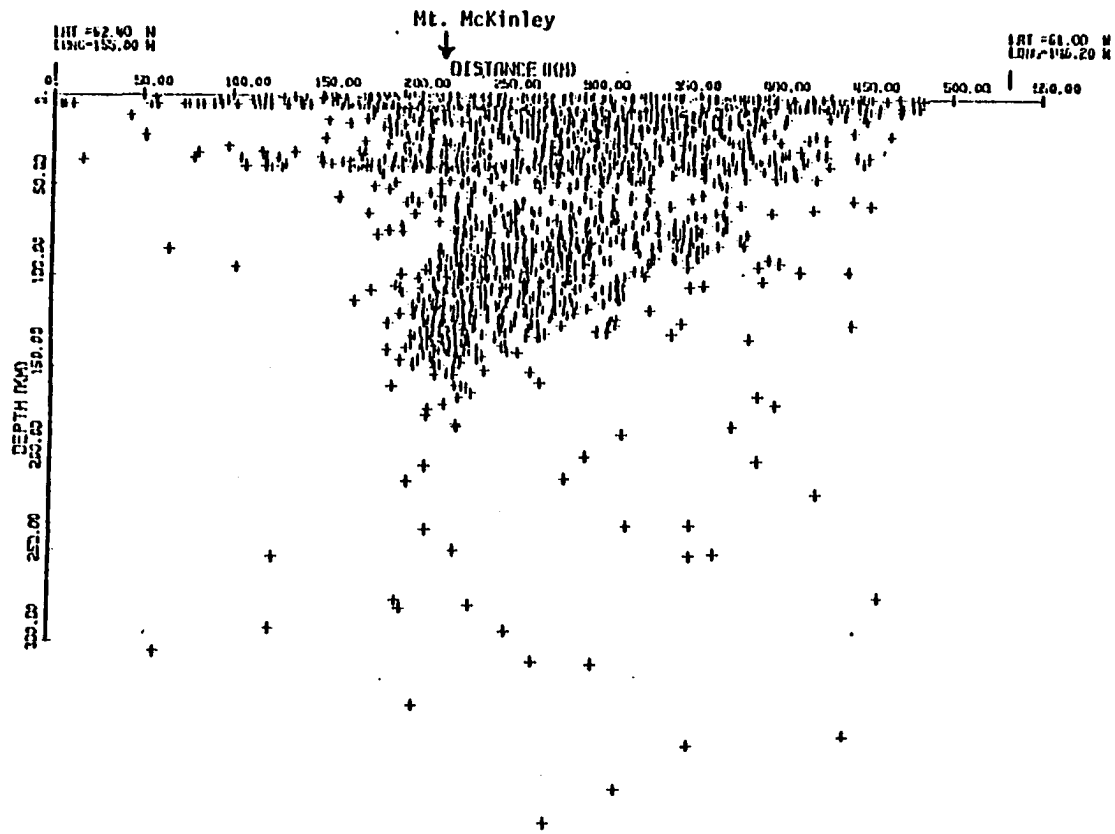


Figure 11 - A vertical plane view of all earthquakes from May 1974 through December 1978, looking N17 E.

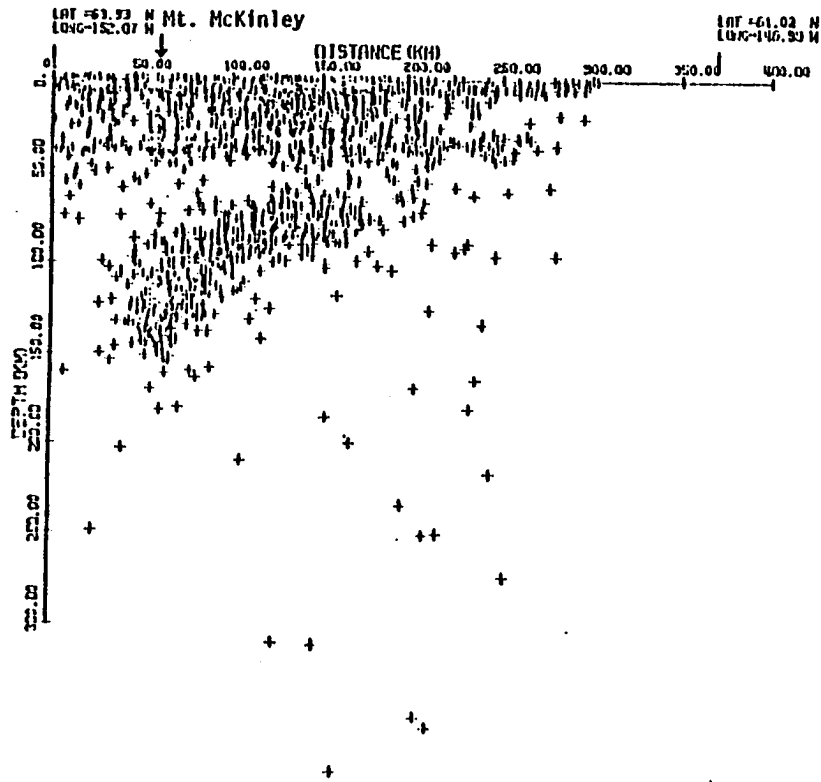


Figure 12 - A vertical plane view of all earthquakes from May 1974 through December 1978, looking N44 E.

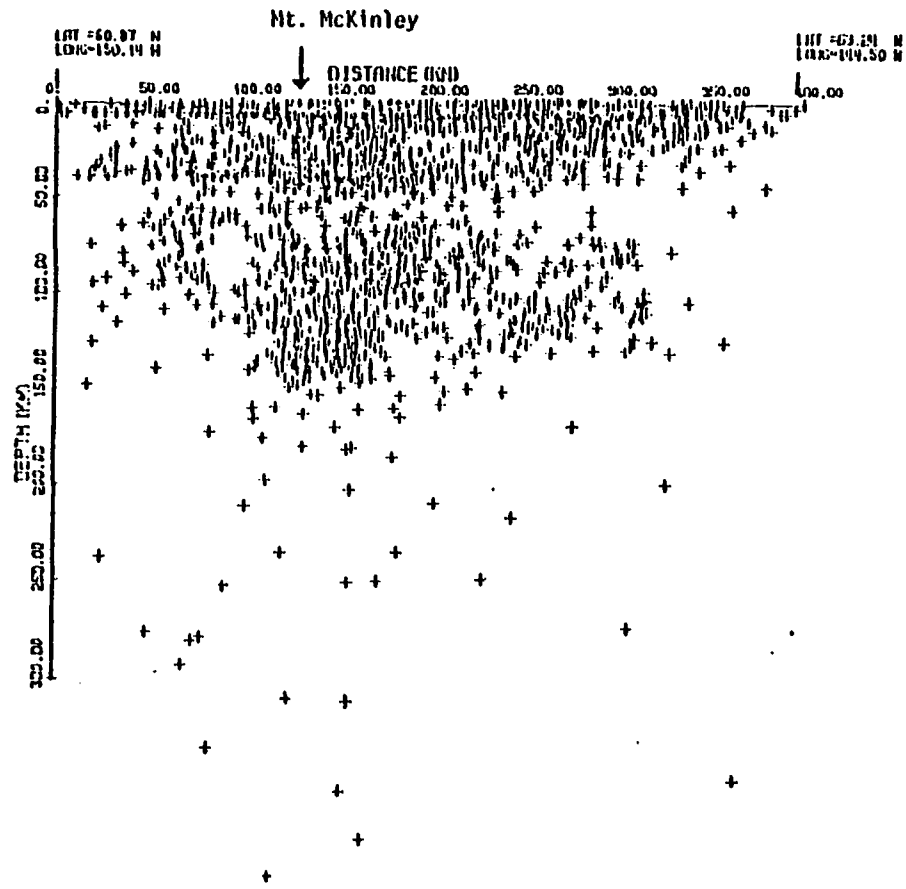


Figure 13 - A vertical plane view of all earthquakes from May 1974 through December 1978, looking N46 W, showing the lateral extent of the Benioff zone.

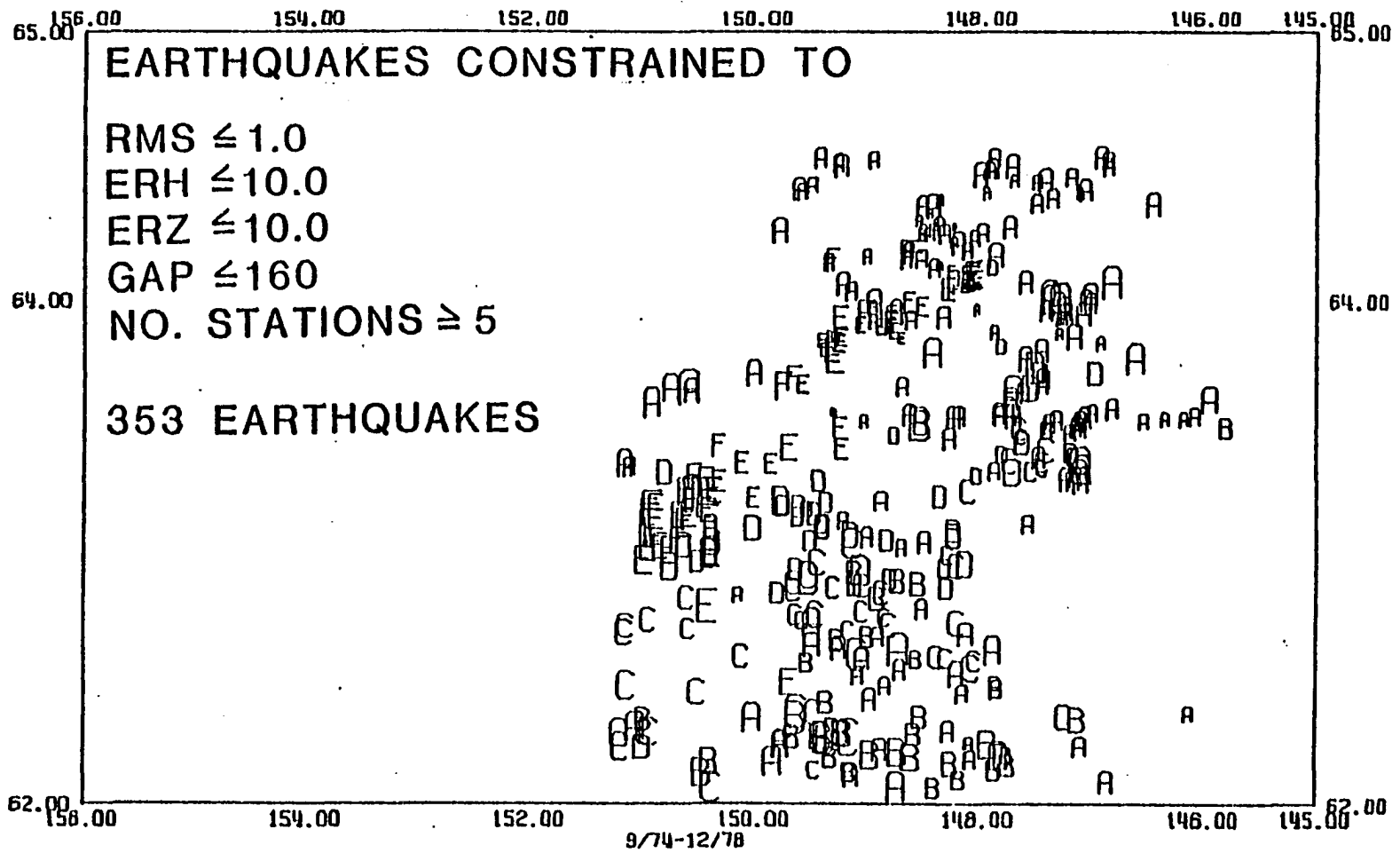


Figure 14 - Locations of all best-fit (constrained) earthquakes in the study area. Letters indicate depth to focus; A = 0-25 km, B = 25-50 km, etc. The size of each letter reflects the magnitude of the earthquake. The events are located at the lower left corner of each letter.

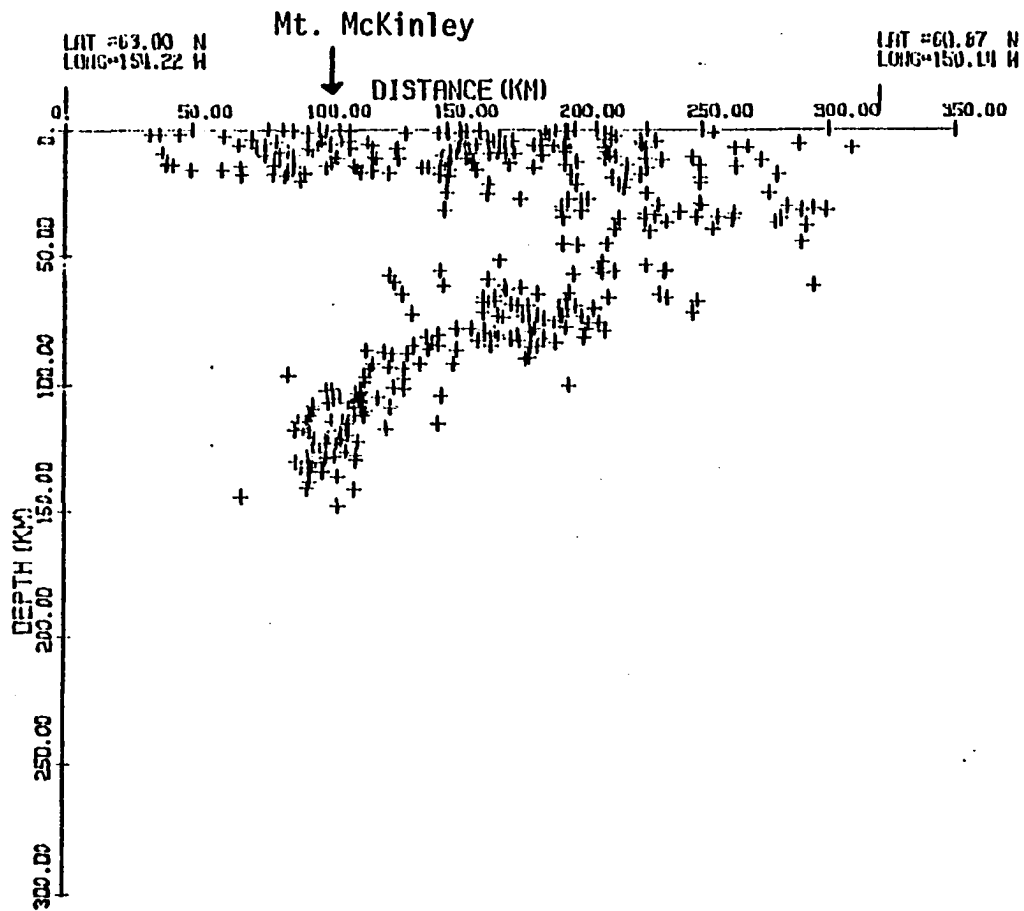


Figure 15 - A vertical plane view of all constrained earthquakes, looking N 52 E, showing the Benioff zone.

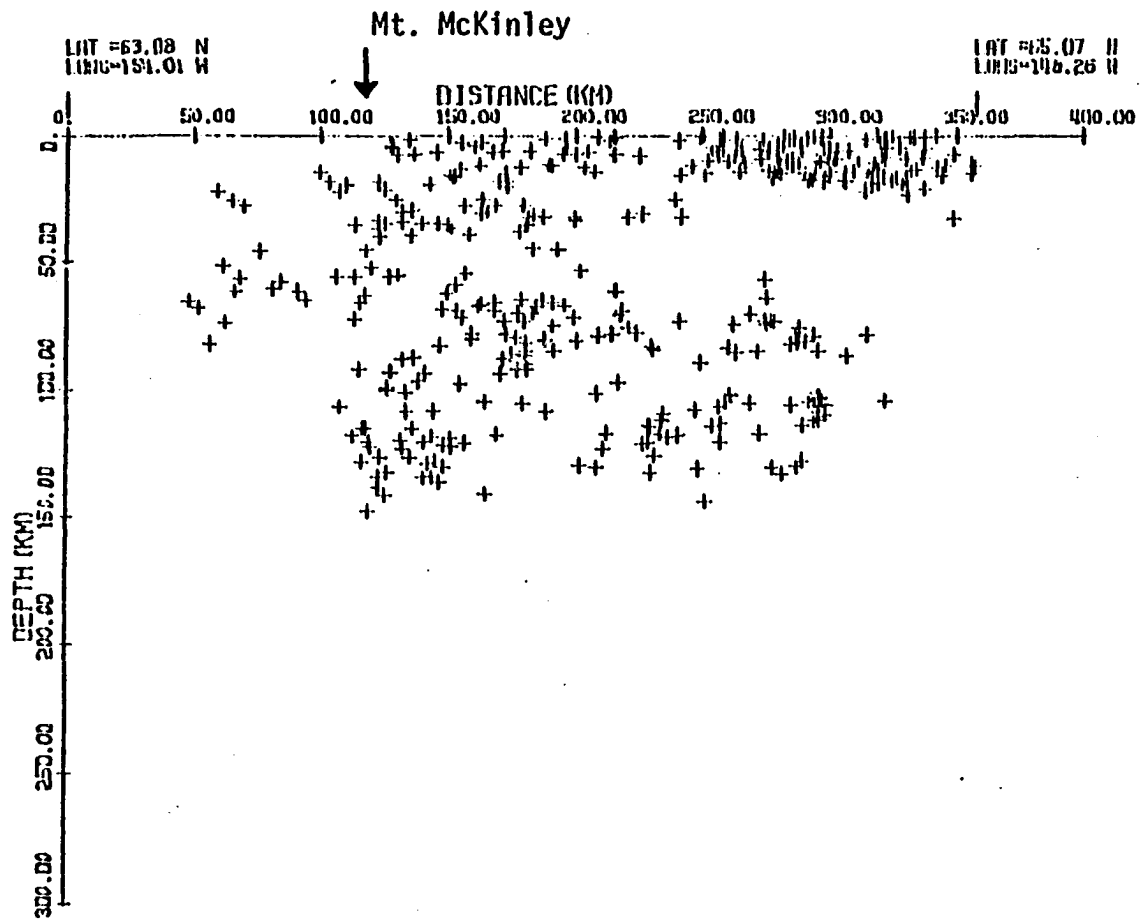


Figure 16 - A vertical plane view of all constrained earthquakes, looking N 38 W, showing the lateral extent of the Benioff zone.

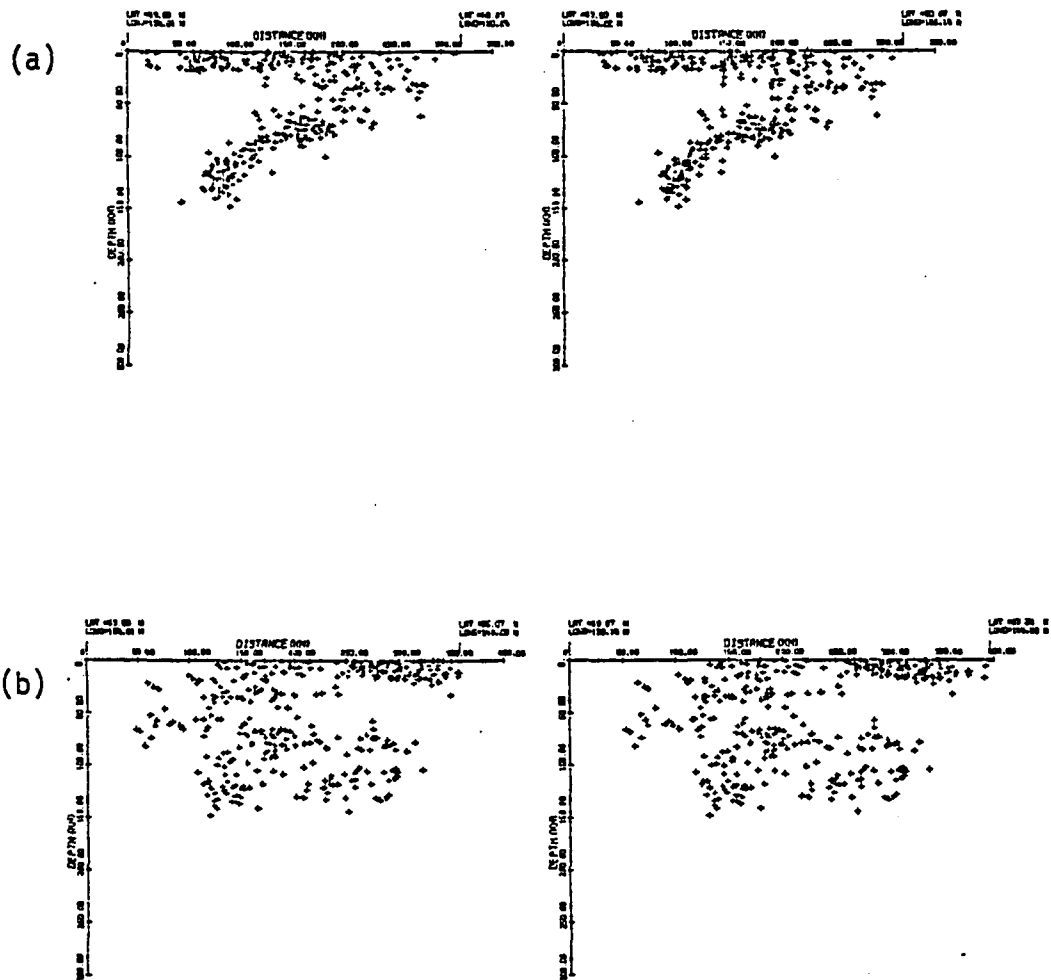


Figure 17 - Stereoscopic pairs of the earthquakes in the Benioff zone showing a three dimensional view along the strike (a) and normal to the strike (b).

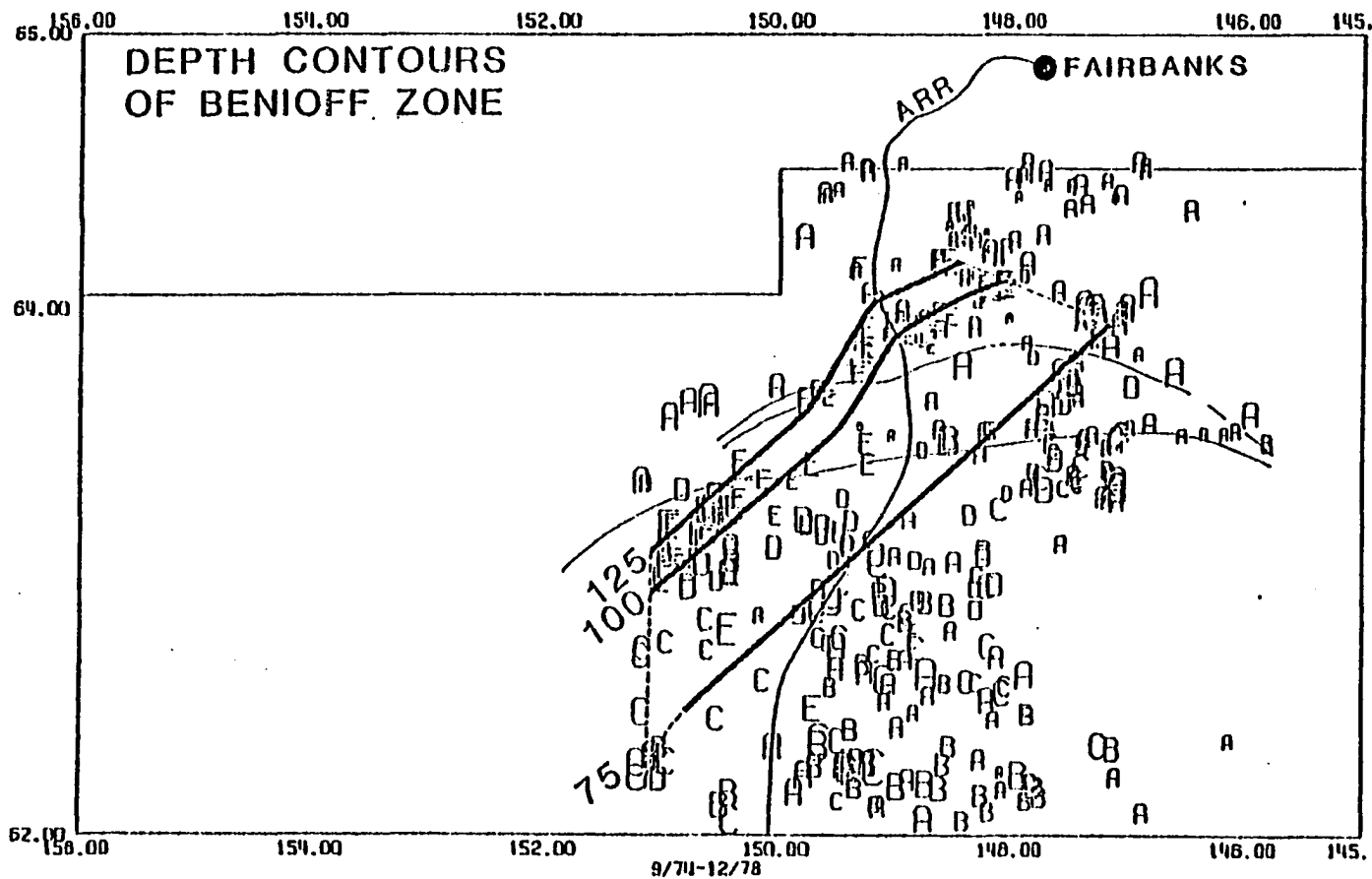


Fig. 18 - Map view of the 75-, 100-, and 125-km depth contours of the top of the Benioff zone superimposed over the constrained earthquakes. Also shown are the Hines Creek and McKinley strands of the Denali Fault. ARR= Alaska Railroad.

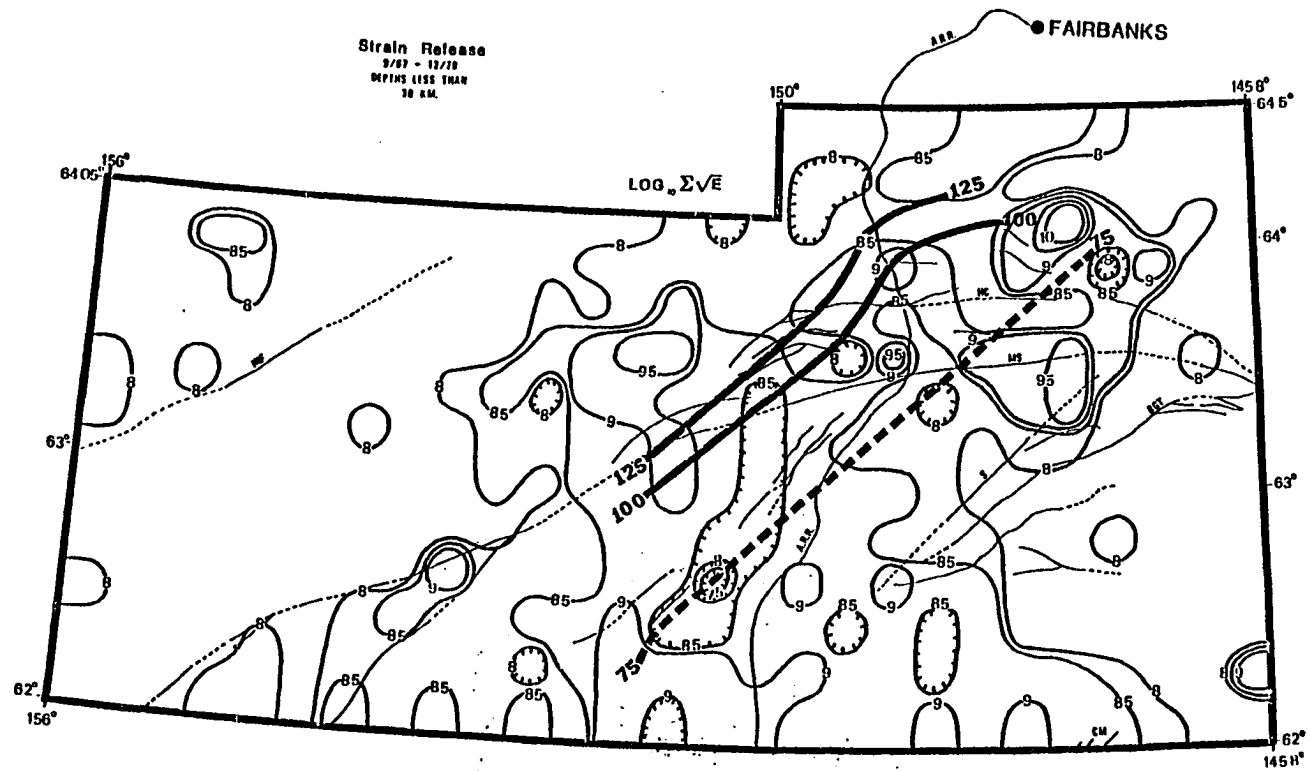


Figure 19 - Strain release for all earthquakes having focal depths of 30 km or less, Sept. 1967 - Dec. 1978. Contour interval in 0.5 units. Hachured contours indicate lower strain release. INF= Iditarod-Nixon fault, HC= Hines Creek strand, MS= McKinley strand, S= Susitna fault, CM= Castle Mountain fault, BGT= Braxson Gulch Thrust fault, ARR= Alaska Railroad. The 75-, 100-, and 125-km depth contours of the Benioff zone are shown in heavy lines.

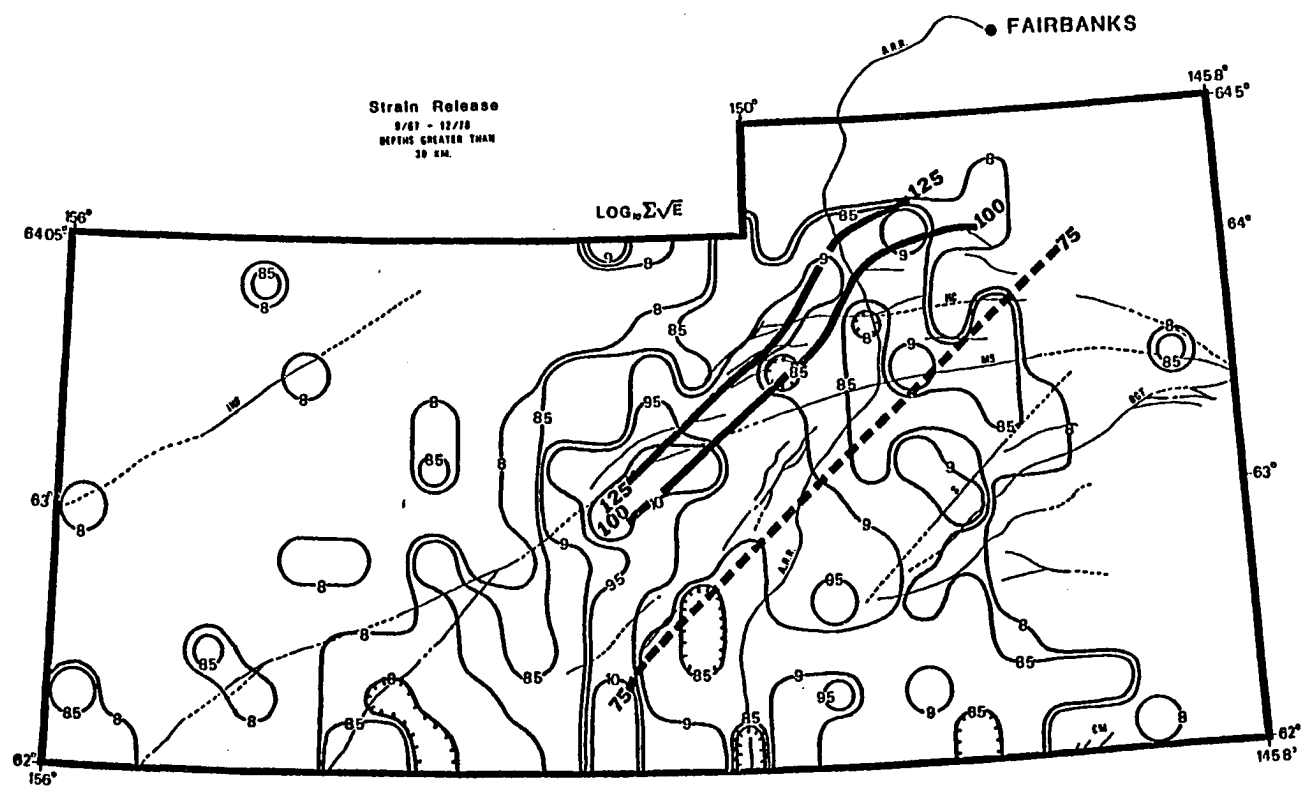


Figure 20 - Strain release for all earthquakes having focal depths greater than 30 km, Sept. 1967 - Dec. 1978.

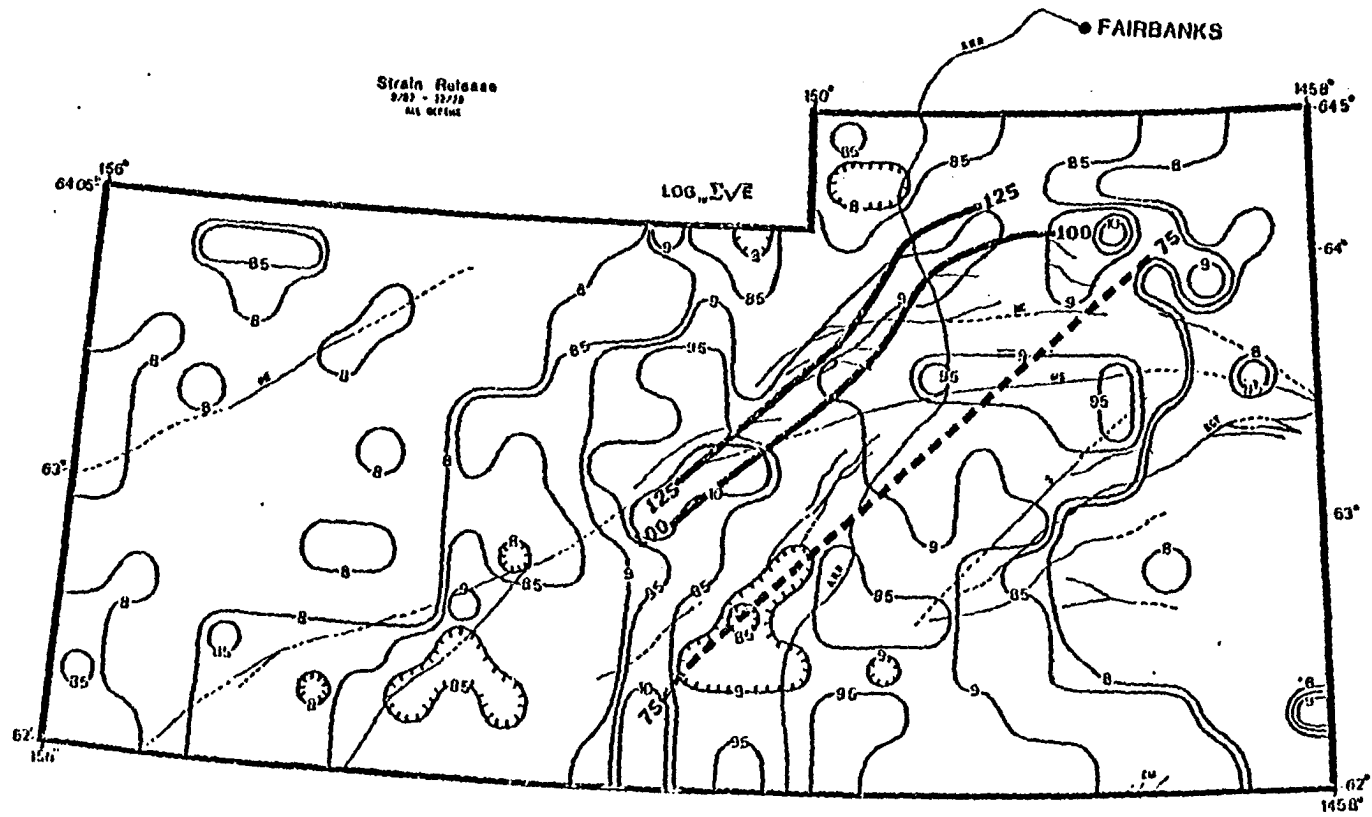


Figure 21 - Strain release for all earthquakes regardless of depth to focus, for September 1967 through December 1978.

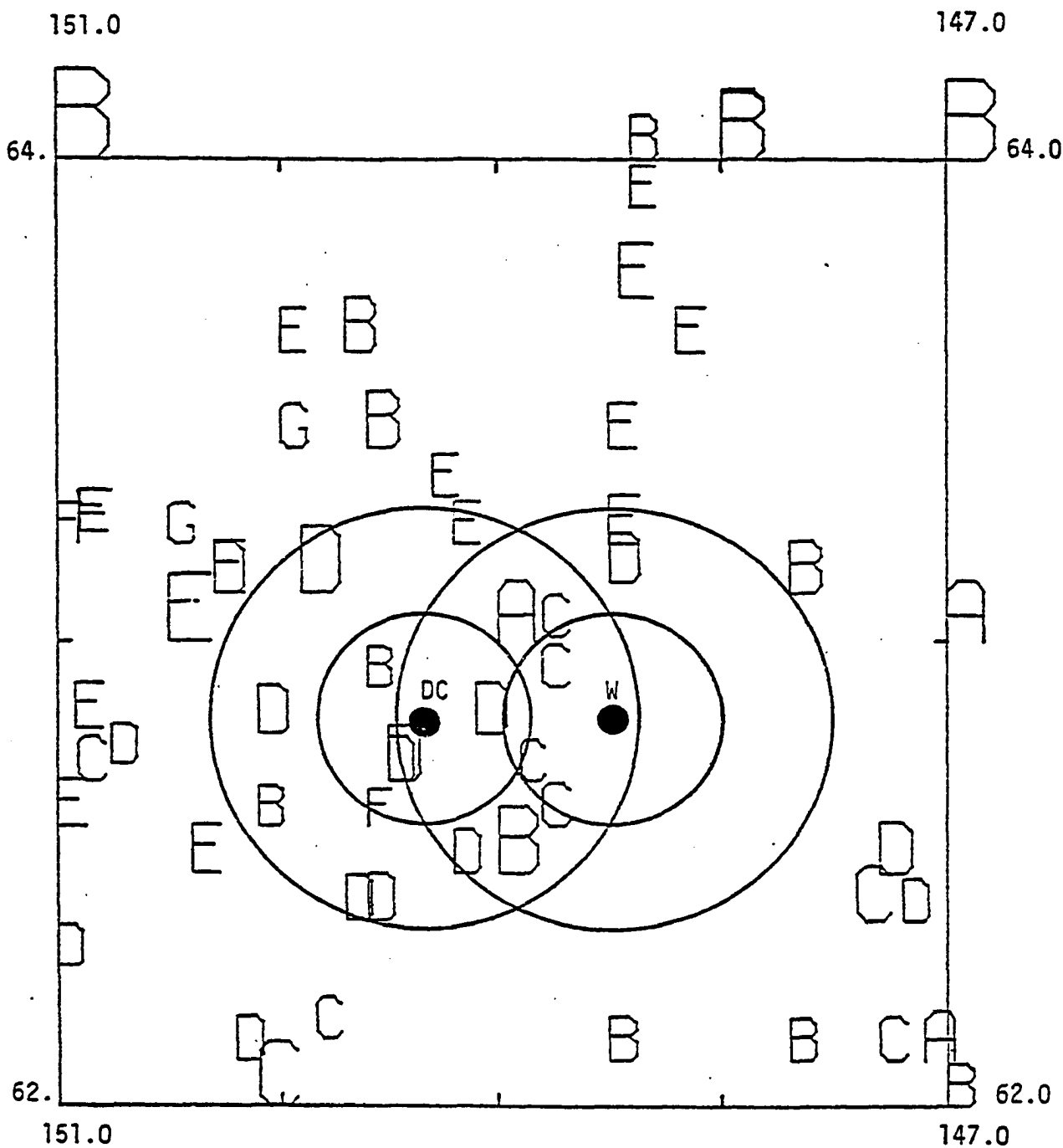


Figure 22 - A map view of all earthquakes of magnitude 3.5 or greater occurring from August 1904 through August 1967. The Devil Canyon and Watana dam sites are shown with 25- and 50-km radii circles drawn in. The size of the letters is proportional to the earthquake magnitude as shown in Figure 25, the largest letter indicating $M \sim 8$.

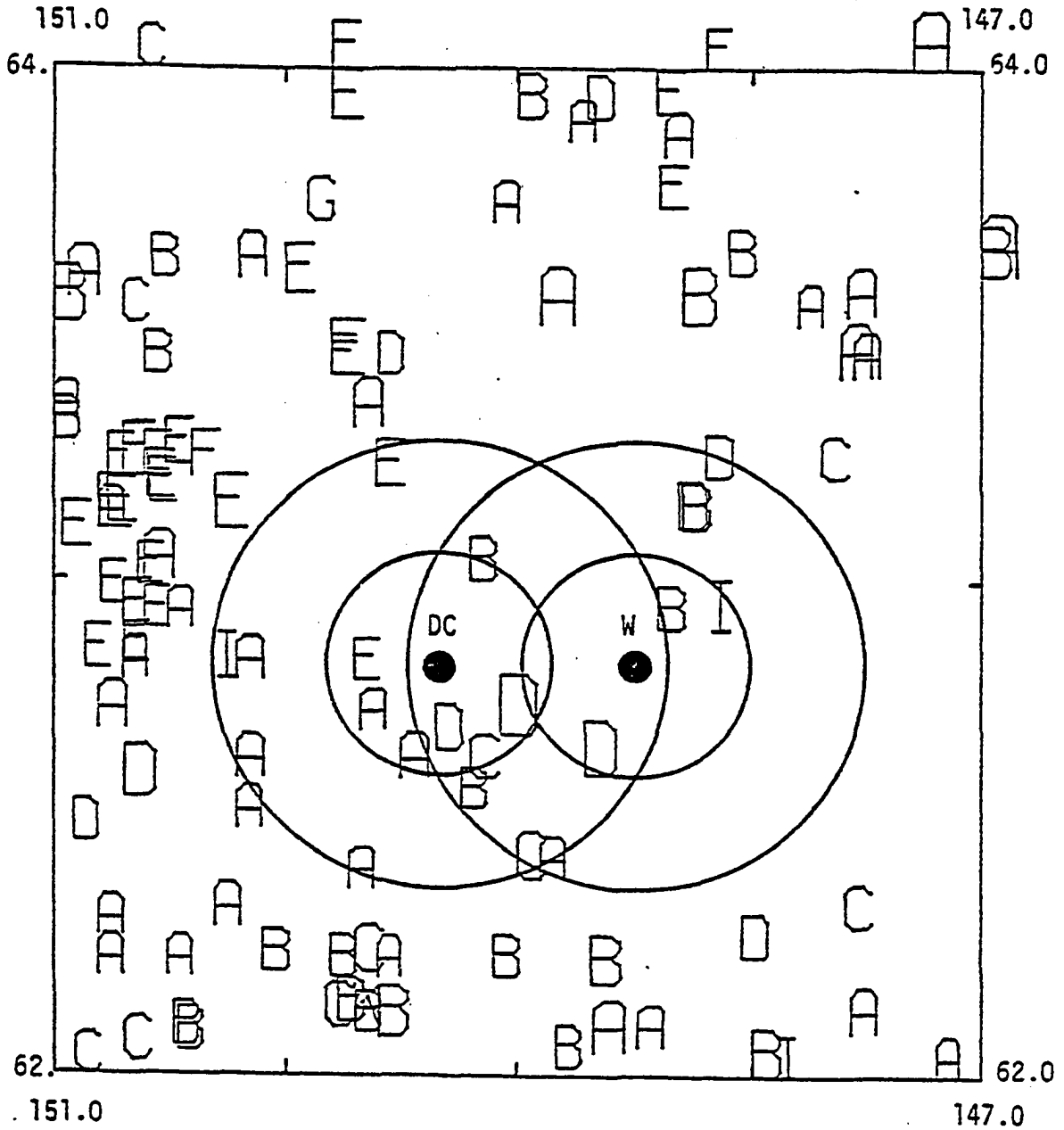


Figure 23 - All earthquakes of magnitude 3.5 or greater occurring from September 1967 through April 1974. The Devil Canyon and Watana dam sites are shown with 25- and 50-km radii circles drawn in. Also, see Figure 25.

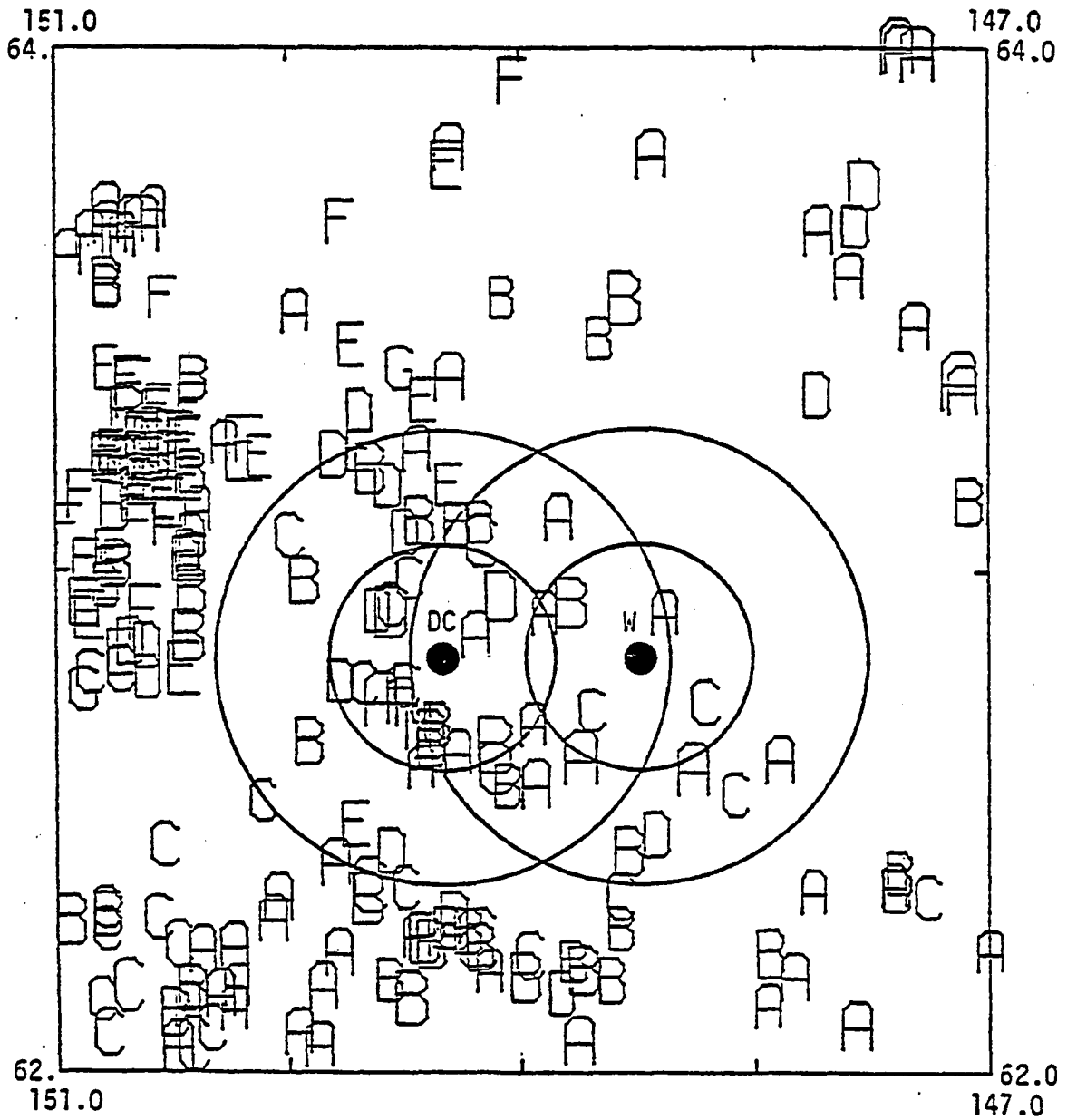


Figure 24 - All earthquakes of magnitude 3.5 or greater occurring from May 1974 through December 1978. The Devil Canyon and Watana dam sites are shown with 25- and 50-km radii circles drawn in. Also, see Figure 25.

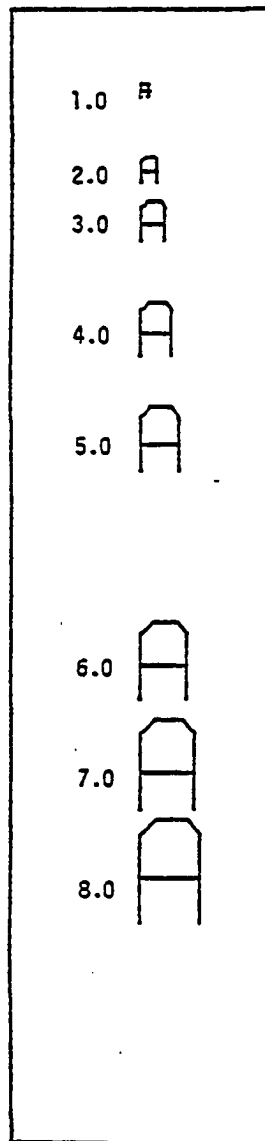


Figure 25 - The relative magnitudes of earthquakes represented by the letters on figures 22, 23 and 24. The numbers beside each letter symbol indicate Richter local magnitude. The earthquakes are located at the lower left corner of each letter.

Table 1

A listing of all earthquakes of magnitude 6.0
or greater within the study area

DATE y/m/d	TIME h/m sec		North Latitude degrees	West Longitude degrees	Depth km	Magnitude
040827	2156	6.0	64- 0.	151- 0.	25.00	8.30
120707	0757	36.0	64- 0.	147- 0.	25.00	7.40
290121	1030	53.0	64- 0.	148- 0.	25.00	6.25
290703	0053	0.	62-30.00	149- 0.	25.00	6.25
290704	0428	35.0	64- 0.	148- 0.	25.00	6.50
320325	2354	51.0	62-30.00	153- 0.	25.00	6.00
320325	2358	31.0	62-30.00	152-30.00	25.00	6.90
320608	0752	39.0	62-30.00	153- 0.	25.00	6.00
350904	0127	39.0	63-45.00	152-30.00	25.00	6.25
480819	1350	46.0	63- 0.	150-30.00	100.00	6.25
620510	0003	40.2	62- 0.	150- 6.00	72.00	6.00
620716	1254	40.6	62-18.00	153- 6.00	39.00	6.00
620818	1643	54.3	62-18.00	152-30.00	32.00	6.13
620818	1746	14.9	62-18.00	152-30.00	32.00	6.38
630502	2313	9.4	63- 6.00	149-54.00	79.00	6.10

Table 2 - Past and present seismometer stations used for earthquake location in the study area.

STATION NAME	CODE	NORTH		WEST		ELEV. METERS	OPENED DATE	DATE CLOSED	CALIBRATED
		LATITUDE DEG MIN	DEG MIN	LONGITUDE DEG MIN	DEG MIN				
ANVIL MOUNTAIN	ANV	64	33.6	165	22.2	327	8/76	----	01/10/77
BARTER ISLAND #1	BI1	70	07.91	143	38.5	10	9/75	8/78	1/1/76
BARTER ISLAND #2	BI2	69	37.43	145	53.57	1097	9/75	8/78	11/19/77
BARTER ISLAND #3	BI3	69	35.2	144	22.26	689	9/75	8/78	11/19/77
BARTER ISLAND #4	BI4	69	31.21	142	58.80	745	9/75	8/78	10/2/77
BROAD PASS	BDP	63	13.90	149	15.49	709	8/71	9/76	
BIRCH HILL	BRH	64	51.89	147	38.42	330	9/70	4/71	
CLEAR CREEK BUTTE	CCB	64	38.88	147	48.32	183	2/71	1/75	
DONNELLY DOME	DDM	63	47.23	145	51.70	920	9/77	----	
DEVIL MOUNTAIN	DMA	66	18.60	164	31.20	243	9/77	----	
ELVEY	ELV	64	51.62	147	50.91	180	8/71	8/72	
ENGINEER HILL	ENG	64	44.11	147	02.76	220	9/71	6/76	
FORT YUKON	FYU	66	33.63	145	12.60	137	2/72	----	1/1/76
FORT YUKON #1	FY1	67	16.00	148	58.17	939	9/75	----	10/11/78
FORT YUKON #2	FY2	67	07.47	147	05.83	671	9/75	----	10/11/78
FORT YUKON #3	FY3	68	08.83	145	42.00	1439	9/75	----	10/12/78
FORT YUKON #4	FY4	67	27.20	146	12.58	792	9/75	----	10/13/78
FORT YUKON #5	FY5	67	08.32	143	14.97	558	9/75	----	10/10/78
GEOPHYSICAL INST	GIA	64	51.60	147	50.10	158	6/69	1/71	
GOLD KING CREEK	GRC	64	10.72	147	56.08	498	7/76	----	4/12/78
GILMORE DOME	GLM	64	59.24	147	23.34	820	8/68	----	05/04/77
HARDING LAKE	HDG	64	24.35	146	57.23	450	9/77	----	9/25/77
HEPP	HPP	64	47.43	147	57.55	170	11/71	6/76	
HURRICANE	HUR	62	58.68	149	38.35	510	8/71	6/75	
KOTZEBUE	KTA	66	51.00	162	36.60	26	8/76	----	10/01/77
LEVY	LVY	64	13.00	149	15.20	230	7/72	----	9/09/77
MOOSE CREEK	MCB	64	43.70	147	12.60	200	9/68	5/70	
MCKINLEY PARK	MCK	63	43.94	148	56.10	610	12/64	----	10/01/77
MERCER	MCR	63	53.71	149	03.56	456	9/71	7/75	
MINITRACK	MIK	64	52.34	147	49.68	160	5/70	3/75	
NENANA	NEA	64	34.63	149	04.63	365	8/71	----	8/20/77
NORTH RIVER	NRA	63	53.40	160	30.60	107	8/76	7/78	10/01/77
PAXSON	PAX	62	58.25	145	28.12	1130	7/69	----	9/28/77
RICHARD D. SIEGRIST	RDS	64	49.59	148	08.68	510	6/77	----	
REMOTE	RON	62	41.48	150	12.23	469	8/71	7/75	
SHEEP CREEK LODGE	SCF	61	59.67	150	02.64	67	8/71	6/75	
SHEEP MOUNTAIN	SCM	61	50.00	147	19.66	1020	6/66	----	9/28/77
SCOTTY LAKE	SCT	62	19.15	150	18.03	140	8/71	6/75	
SUNSHINE	SSH	62	10.00	150	04.66	100	8/71	9/72	
SAVOONGA	SVG	63	41.40	170	28.80	15	8/77	----	10/01/77
TIN CITY	TNA	65	33.60	167	55.20	76	10/76	----	10/01/77
TANANA	TNN	65	15.40	151	54.70	504	1/65	----	10/24/70
UNALAKLEET	UNL	63	53.65	160	40.60	122	6/78	----	10/02/78

N.O.A.A. STATIONS RECEIVED AT THE GEOPHYSICAL INSTITUTE

BLACK RAPIDS	BLR	63	30.10	145	50.70	809	3/65	----	
GILMORE	GIL	64	58.50	147	29.70	350	10/67	----	
GRANITE MOUNTAIN	GMA	65	25.72	161	13.91	858	9/70	----	
INDIAN MOUNTAIN	IMA	66	04.11	153	40.72	1380	8/71	----	
PALMER OBSERVATORY	PMR	61	35.53	149	07.85	100	9/67	----	
ARCTIC VALLEY	PMS	61	14.68	149	33.63	716	5/67	----	
PALMER WEST	PWA	61	39.05	149	52.72	137	5/67	----	
SPARREVOHN	SVW	61	06.49	155	37.30	762	8/67	----	
TOLSONA	TOA	62	06.28	146	10.34	909	9/71	----	
TATALINA	TTA	62	55.80	156	01.31	914	8/72	----	

Table 3 - Quality of earthquake locations during the epoch
 May 1974 to December 1978 using HYP071.
 RMS= Root-mean-square travel-time error in seconds
 #STATIONS= Number of stations used to locate the event
 ERH= Horizontal location error in km
 ERZ= Vertical error in km

RMS	#EVENTS	%TOTAL	#STATIONS	#EVENTS	%TOTAL
≤ 0.1	446	18.1	≤ 3	168	5.8
0.2	726	29.5	≤ 4	655	26.6
0.3	1045	42.5	5	1039	44.3
0.4	1336	54.3	6	1389	56.4
0.5	1584	64.4	7	1594	64.8
0.6	1772	72.0	8	1758	71.4
0.7	1910	77.6	9	1935	78.6
0.8	2013	81.8	10	2058	83.6
0.9	2114	85.9	15	2303	93.6
1.0	2118	83.9	20	2398	97.4
2.0	2384	96.9	25	2453	99.7
3.0	2415	98.1	30	2458	99.9

ERH	#EVENTS	%TOTAL	ERZ	#EVENTS	%TOTAL
≤ 1	697	28.3	≤ 1	697	28.3
2	814	33.1	2	732	29.7
3	1056	42.9	3	813	33.0
4	1261	51.2	4	927	37.7
5	1429	58.1	5	1042	42.3
6	1556	63.2	6	1134	46.1
7	1657	67.3	7	1230	50.0
8	1736	70.5	8	1321	53.7
9	1795	72.9	9	1387	56.4
10	1850	75.2	10	1449	58.9
15	2041	82.9	15	1653	67.2
20	2140	87.0	20	1750	71.1
25	2207	89.7	25	1814	73.7
30	2256	91.7	30	1859	75.6
40	2320	94.3	40	1906	77.4
50	2347	95.4	50	1939	78.8
			60	1970	80.0
			70	1992	80.9
			100	2045	83.1
			200	2111	85.8
			300	2144	87.1
			400	2172	88.3
			500	2205	89.6

Table 3 (cont'd) - Quality of earthquake locations during the epoch May 1974 to December 1978.

GAP= Largest azimuthal angle between stations, in degrees
 DMIN/DEPTH= Ratio of distance to nearest station divided by focal depth of earthquake

DEPTH= Focal depth of earthquake in km

The DEPTH table includes 111 events from the Meyer catalog which had no estimates of ERH, ERZ, GAP, or DMIN/DEPTH.

GAP	#EVENTS	%TOTAL	DMIN/DEPTH	#EVENTS	%TOTAL
≤30	0	0.0	≤1	495	20.1
40	3	0.1	2	923	37.5
50	14	0.6	3	1075	43.7
60	55	2.2	4	1199	48.7
70	89	3.6	5	1371	55.7
80	130	5.3	6	1488	60.5
90	160	6.5	7	1568	63.7
100	199	8.1	8	1625	66.0
110	248	10.1	9	1663	67.6
120	313	12.7	10	1694	68.8
130	413	16.8	20	1905	77.4
140	500	20.3	30	2021	82.1
150	594	24.1	40	2097	85.2
160	694	28.2	50	2184	83.7
			60	2243	91.1
			70	2293	93.2
			80	2323	94.4
			90	2351	95.5
			100	2372	96.4

DEPTH	#EVENTS	%TOTAL
≤ 5	779	30.3
10	915	35.6
20	1126	43.8
30	1287	50.0
40	1528	53.3
50	1698	66.0
60	1736	67.5
70	1803	70.1
80	1899	73.8
90	2017	78.4
100	2122	82.5
110	2227	86.6
120	2328	90.5
130	2425	94.3
140	2495	97.0
150	2523	98.1
175	2540	98.8
200	2547	99.0

Table 4

Velocity model used for Group III earthquakes,
May 1974 to December 1978

<u>DEPTH (KM)</u>	<u>VELOCITY OF P-WAVE (KM/SEC)</u>
0.0 - 24.3	5.90
24.4 - 40.1	7.40
40.2 - 75.9	7.90
76.0 - 300.9	8.29
301.0 - 544.9	10.40
545.0 - ∞	12.60

Table 5

Comparison of depths of earthquakes using P, then P and S first motions. MAG - magnitude of the earthquake. Z(P) - depth of focus using only the P-arrival, in km. Z(P,S) - depth of focus using both the P and S arrivals, in km. DZ - difference in the depth estimate, in km. RMS(P) - residuals for P-arrivals only, in seconds. RMS(P,S) - residuals for both P and S arrivals, in seconds. DRMS - difference in the residuals, in seconds.

* - Only three stations used in the location.

** - Only four stations used in the location.

DATES	TIME	MAG	Z(P)	Z(P,S)	DZ	RMS (P)	RMS (P,S)	DRMS
740507	2258	1.85	4.52	2.66	-1.86	0.16	0.94	+0.69
740516	1055	3.50	92.59	61.85	-20.73	0.28	0.67	+0.39
740525*	0245	1.45	5.00	93.55	+88.55	0.00	0.00	---
740804**	2310	1.87	112.35	110.12	-2.23	0.00	0.19	---
741002	2325	2.07	103.57	104.93	+1.36	0.04	0.07	+0.03
750522	2139	2.80	2.76	2.55	-0.20	0.27	0.30	+0.03
750528	1528	2.65	105.69	63.29	-42.40	0.24	0.76	+0.52
750529	0323	2.40	11.24	12.90	+1.66	0.44	0.95	+0.51
750702*	0155	2.85	53.65	88.77	+25.11	0.05	0.00	---
750705	0522	2.34	85.09	117.80	+31.71	0.00	0.00	---
750721	2309	2.23	32.20	45.22	+13.02	0.25	0.23	-0.02
750724	0139	2.42	114.39	122.53	+8.14	0.29	0.20	-0.09
750304	0419	3.06	59.68	50.70	-18.98	0.23	0.49	+0.25
750805**	0457	2.48	4.50	5.00	+0.50	0.30	0.39	+0.09
750307	0937	2.53	109.93	5.03	-104.9	0.04	1.26	+1.22
751204	0715	2.67	59.85	32.99	-30.86	0.35	0.70	+0.35
751210**	0205	1.11	7.48	0.63	-6.85	0.00	1.13	---
751211	1148	2.90	1.47	3.64	+2.17	0.38	0.55	+0.17
751211	2153	1.68	12.11	17.55	+5.44	0.21	0.36	+0.15
751215	2005	2.70	7.28	3.76	-3.52	0.50	0.63	+0.13
751218	0000	3.80	100.61	32.51	-68.10	0.05	0.61	+0.56
751227	0131	3.21	31.35	44.95	+13.59	0.22	1.97	+1.75
751227	0922	3.52	12.96	15.01	+2.05	0.47	0.91	+0.44
751205*	2254	2.47	5.00	25.85	+21.85	0.00	0.15	---
761219	2008	3.49	138.40	116.04	-22.36	0.27	0.37	+0.10
770105*	1538	1.97	5.00	22.70	+17.70	0.01	0.26	---
770117**	0857	2.90	0.11	32.96	+32.85	0.48	1.42	---
770305	2117	2.01	15.10	18.83	+3.73	0.15	0.42	+0.27
770410	1037	1.31	128.12	104.00	-24.12	0.00	0.28	+0.28
780128	0219	3.37	129.50	127.74	-1.75	0.28	0.29	+0.01
780128	1933	2.78	105.86	112.42	+6.56	0.30	0.29	-0.01
780214	1430	3.39	73.95	67.22	-6.74	0.20	1.01	+0.81
780318	0643	3.19	0.43	2.98	+2.55	0.54	0.92	+0.28
780409	2358	3.29	130.96	124.98	-5.98	0.23	0.43	+0.20
780717	1710	3.18	104.88	102.51	-2.37	0.14	0.17	+0.03
780717	1801	1.45	102.43	109.54	+7.11	0.17	0.23	+0.06
780723	1703	4.15	10.46	10.99	+0.53	0.49	0.43	-0.06
780729	0225	2.79	9.04	8.45	-0.59	0.40	0.51	+0.11
780729	2155	2.36	0.09	11.47	+11.38	0.22	0.44	+0.22
780304	0207	3.88	45.85	48.37	+2.52	0.43	0.44	+0.01
780824	0338	3.12	118.15	117.19	-0.96	0.12	0.18	+0.06

Table 6

Average depth of Geophysical Institute locations compared to NOAA locations, in km

YEAR	NO. EVENTS	AVE. G.I. IS:	STD. DEVIA.
1974	62	18 KM DEEPER	81 KM
1975	90	2 KM SHALLOWER	59 KM
1976	48	36 KM SHALLOWER	39 KM
1977	44	37 KM SHALLOWER	38 KM

Table 7 - Sliding window of 200 events and the b-slope for each group for the time period September 1967 through December 1978. Groups overlap by 100 events.

DATES	TOTAL EVENTS	EVENTS M>2.9	B SLOPE	ST.DEV.	MMAX
670901 - 680319	200	44	0.76	0.50	5.3
671218 - 680517	200	30	0.87	0.42	4.8
680319 - 680723	200	27	1.47	0.25	4.0
680517 - 681012	200	22	1.35	0.25	4.0
680723 - 681221	200	22	1.19	0.29	4.1
681014 - 690212	200	24	1.53	0.27	4.5
681221 - 690330	200	19	1.42	0.29	4.5
690212 - 690525	200	29	0.95	0.41	5.0
690331 - 690925	200	52	0.89	0.44	5.1
690525 - 691125	200	49	0.95	0.42	5.1
690925 - 700205	200	37	1.36	0.31	5.1
691127 - 700410	200	36	1.38	0.26	4.0
700205 - 700513	200	25	0.95	0.41	5.0
700410 - 700513	200	22	1.27	0.33	5.0
700513 - 700918	200	23	1.31	0.29	4.3
700519 - 701027	200	20	0.80	0.35	4.3
700919 - 701214	200	20	0.53	0.58	5.6
700123 - 710307	200	35	0.50	0.64	5.6
701215 - 710515	200	56	0.63	0.54	5.4
710307 - 710925	200	63	1.11	0.32	4.3
710516 - 711111	200	48	1.09	0.35	4.6
710925 - 711211	200	36	1.18	0.33	4.6
711111 - 720129	200	50	1.55	0.23	3.9
711211 - 720305	200	74	1.83	0.19	3.7
720129 - 720408	200	79	2.25	0.17	3.7
720305 - 720427	200	65	1.50	0.28	4.6
720408 - 720516	200	54	1.09	0.35	4.6
720427 - 720517	200	62	1.95	0.21	4.2
720516 - 720721	200	77	2.15	0.20	4.8
720517 - 720721	200	70	1.59	0.27	4.8
720721 - 720923	200	43	1.53	0.22	3.8
720322 - 721105	200	22	0.85	0.46	5.2
720923 - 721227	200	19	0.59	0.51	5.2
721105 - 730205	200	18	1.04	0.30	4.1
721229 - 730315	200	22	1.41	0.24	3.9
730205 - 730507	200	28	1.18	0.33	4.6
730315 - 730527	200	28	0.94	0.38	4.6
730507 - 730824	200	21	0.89	0.30	4.0
730527 - 731030	200	24	1.12	0.33	4.4
730824 - 731231	200	34	1.45	0.28	4.4
731030 - 740313	200	44	1.02	0.37	4.7

Table 7 (continued)

DATES	EVENTS TOTAL	EVENTS M>2.8	B SLOPE	ST. DEV	MMAX
740101 - 740519	200	46	0.83	0.40	4.7
740315 - 740706	200	55	1.09	0.36	4.7
740520 - 740902	200	73	1.11	0.35	4.6
740708 - 741111	200	73	1.09	0.33	4.4
740902 - 750108	200	83	1.03	0.34	4.4
741112 - 750310	200	93	0.87	0.37	4.4
750109 - 750522	200	114	0.84	0.47	5.4
750311 - 750723	200	95	0.95	0.43	5.4
750523 - 750917	200	78	1.22	0.32	4.5
750724 - 751211	200	103	1.03	0.31	4.2
750917 - 750218	200	125	0.94	0.33	4.2
751211 - 750407	200	124	0.93	0.37	4.5
750219 - 750501	200	129	1.00	0.35	4.5
750403 - 770102	200	131	0.75	0.45	4.9
750502 - 770322	200	112	0.65	0.49	4.9
770103 - 770515	200	92	0.93	0.37	4.5
770322 - 770702	200	105	1.11	0.30	4.1
770515 - 770830	200	82	0.97	0.37	4.5
770703 - 771025	200	59	0.99	0.37	4.5
770330 - 771221	200	52	1.15	0.33	4.5
771025 - 780305	200	77	0.91	0.35	4.3
771222 - 780509	200	100	0.93	0.37	4.5
780305 - 780715	200	109	0.93	0.43	5.2
780510 - 780808	200	103	0.88	0.45	5.2
780716 - 781001	200	93	0.84	0.42	4.8
780808 - 781215	200	81	0.85	0.40	4.6
781003 - 781231	147	46	0.99	0.37	4.6

Table 8 - All earthquakes of magnitude 3.5 or greater within approximately 50 km of the proposed Susitna dam sites.

DATE	TIME	N. LAT.	W. LONG	DEPTH	DMIN					
y/m/d	h/m sec	deg/min	d/m	km	Mag	N	GAP	RMS	ERH	ERZ
290703	053	0.	62-30.00	149- 0.	25.00	6.25				
310529	516	32.0	63- 0.	149- 0.	0.	5.50				
630502	2313	9.4	63- 6.00	149-54.00	79.00	6.10				
630922	358	43.2	63-12.00	148-30.00	101.00	4.50				
630922	2033	47.7	62-54.00	148-48.00	53.00	4.00				
631019	1119	31.8	62-24.00	149-35.00	95.00	4.30				
631214	751	7.9	62-42.00	149-30.00	95.00	5.10				
640906	1736	44.3	63- 5.00	147-42.00	33.00	4.90				
641221	1932	3.0	63- 6.00	150-18.00	111.00	4.20				
650509	1427	18.5	63-12.00	149-12.00	111.00	4.00				
650626	2315	42.4	62-48.00	149- 5.00	75.00	4.80				
651016	1145	25.7	63- 5.00	150-18.00	84.00	4.60				
651118	1539	47.3	62-36.00	150- 5.00	33.00	3.90				
651224	1610	1.1	62-24.00	149-42.00	95.00	4.20				
650105	11 0	5.9	62-35.00	149-35.00	131.00	3.50				
650110	5 1	22.5	62-42.00	148-54.00	57.00	3.70				
650511	126	24.3	62-48.00	150- 5.00	99.00	4.60				
650505	11 9	13.5	62-54.00	149-35.00	45.00	3.90				
650618	631	41.0	63-18.00	149-18.00	108.00	3.90				
651011	1549	49.2	62-35.00	148-48.00	54.00	4.20				
670331	418	31.3	63- 7.44	148-29.70	92.00	4.50				
670410	1444	25.8	63- 0.48	148-47.92	72.00	4.00				
670514	2045	44.7	62-30.00	149-12.00	95.00	4.10				
670712	1515	37.9	62-42.00	149-30.00	78.00	4.10				
670923	4 2	43.2	62-24.00	148-54.00	23.00	3.60	4	0.90		
680116	2044	25.3	63-12.00	147-42.00	50.00	3.70	3	0.00		
680307	15 5	0.1	62-35.00	150-12.00	9.00	3.80				
680902	1321	30.5	62-48.00	150-12.00	5.00	3.70	5	0.40		
681228	415	44.2	62-54.00	148-12.00	210.00	4.50	5	0.40		
690528	10 7	14.2	62-30.00	150-12.00	0.00	3.60	5	0.30		
690509	8 2	17.2	62-24.00	149- 0.	54.00	4.10				
690621	1739	33.4	63- 0.00	149-12.00	40.00	3.70	8	0.30		
691207	328	57.5	63-11.10	149-35.05	104.00	3.90				
700309	1149	11.9	62-35.00	149-30.00	0.00	4.00	8	0.40		
700312	1145	12.3	62-54.00	148-24.00	40.00	3.80	9	0.30		
700917	240	26.6	62-48.00	150-18.00	200.00	3.90	11	0.40		
710221	1810	35.5	63- 6.00	150-18.00	100.00	4.70	9	0.20		
710516	1650	57.4	63- 6.18	148-18.96	77.00	4.10				
710516	1650	57.4	63- 6.00	148-18.00	40.00	4.10	8	0.50		
710726	1617	35.6	63-18.00	149-42.00	15.00	4.10		0		
710821	2235	50.2	62-43.00	149-42.00	100.00	3.50		0		
711011	1848	39.6	63-12.00	148-12.00	91.00	3.90	18	0.50		
711125	1541	42.4	62-35.00	149-12.00	74.00	3.90		0		
720330	1425	14.4	62-42.00	149-40.20	15.00	3.50	18	0.40		
720325	1243	30.8	62-22.80	149-43.20	15.00	3.50	13	0.90		
721001	10 8	50.9	62-41.40	149- 4.20	75.00	5.20	22	0.30		
730822	8 2	16.0	62-39.60	149-21.00	75.00	3.90	16	0.30		
740205	225	23.1	62-35.60	148-42.60	75.00	4.70	20	1.00		
740305	1025	59.3	62-32.40	149-14.40	40.00	3.50	13	0.70		
740524	2120	20.95	63-11.20	149-43.99	119.87	3.50	16	97	72.7	1.53 10.5 24.6 C1
740525	523	29.47	63- 7.29	149-21.21	120.21	3.50	16	68	71.2	3.19 20.1 49.0 C1
741225	317	33.35	62-38.80	149-29.30	311.37	3.66	7	152	55.5	1.18 37.1 46.7 D1
750107	19 8	51.35	62-52.35	148-57.02	8.08	8.55	6	120	57.1	0.68 22.3 52.5 D1

Table 8 (continued)

DATE	TIME	N. LAT.	W. LONG	DEPTH	DMIN								
y/m/d	h/m sec	deg/min	d/m	km	Mag	N	GAP	RMS	ERH	ERZ			
750109	2014	9.54	52-43.62	149-32.39	59.90	3.53	9	90	34.2	0.24	2.9	4.7	B1
750110	523	31.5	53- 1.55	150- 2.28	74.00	3.50							
750215	742	30.02	53-17.04	149-27.89	104.07	3.61	7	155	75.9	0.09	1.9	3.5	C1
750305	337	49.45	53-15.76	149-44.30	85.52	3.55	5	274	109.0	0.01	2.9	2.7	D1
750515	445	32.30	52-55.91	149-59.87	37.39	3.90	12	116	132.7	0.39	2.5	430.0	D1
750518	1542	59.1	53-10.20	150-15.78	105.00	5.40							
750529	855	21.5	52-43.92	149-43.08	51.00	3.50							
750705	745	54.0	52-25.80	149-28.62	75.00	3.70							
751113	2025	55.81	52-31.55	149- 6.58	37.91	3.65	5	170	89.8	0.20	5.2	6.9	D1
751116	1835	55.35	52-52.20	148-25.32	0.67	3.65	11	115	118.5	0.62	4.7	8.9	D1
751218	0 0	2.00	52-25.97	149-45.01	100.61	3.80	5	155	144.7	0.05	1.5	5.3	O1
751227	922	25.77	52-35.76	149-19.07	12.95	3.52	12	135	101.7	0.47	3.5	4.8	D1
750109	2145	26.42	52-43.65	149-33.94	17.52	3.55	5	195	120.8	0.53	3.9	52.4	O1
750119	2127	37.11	52-49.70	149-14.58	19.44	3.70	11	135	123.1	0.12	1.3	17.4	D1
750205	339	50.23	52-34.11	149-29.75	3.55	3.51	5	189	103.4	1.17	50.8	99.8	D1
750219	530	14.89	53- 8.70	149-42.09	35.95	4.29	19	55	155.8	0.53	2.4	594.8	D1
750219	1145	32.45	52-33.94	149-24.39	43.19	3.61	9	111	114.0	0.31	3.0	53.8	D1
750223	1018	37.11	52-34.75	147-57.04	13.97	3.90	12	100	99.2	0.43	3.3	4.3	D1
750317	2238	53.25	52-31.65	148-59.70	1.43	4.00	5	171	108.0	0.94	6.6	12.3	D1
750322	1159	55.72	52-23.54	148-35.89	32.29	4.04	11	94	53.7	0.44	5.9	20.8	D1
750408	2129	14.92	53- 2.71	149-19.30	25.03	3.74	5	138	155.1	0.35	5.5	20.5	D1
750416	1857	55.98	52-35.55	149-25.93	27.59	3.79	9	127	75.5	0.58	8.2	30.1	D1
750519	1921	54.50	53-11.34	149-29.75	7.14	3.79	6	141	172.5	1.18	6.7	112.7	D1
750521	2315	45.59	53-12.19	150-19.30	3.25	3.60	21	84	135.5	0.51	2.5	29.9	D1
750503	1735	47.40	52-41.58	149-34.16	15.10	3.90	7	135	81.9	0.13	1.5	2.0	C1
750508	225	33.72	52-33.30	148-19.53	0.34	4.35	5	108	95.8	0.27	11.8	24.7	D1
750511	14 5	44.10	52-53.05	149-50.73	32.97	4.29	5	115	115.9	0.39	7.8	25.4	D1
750715	8 9	45.49	52-41.32	149-39.72	0.15	4.6	9	142	116.2	0.99	18.0	123.9	D1
750929	1347	20.6	52-30.00	150- 9.35	59.00	3.50							
751024	1719	54.28	52-35.61	149-10.71	37.65	4.8	11	101	111.2	0.29	2.5	359.6	D1
751227	12 4	49.55	52-53.81	149- 8.53	90.54	4.24	15	131	93.7	0.30	2.1	4.7	C1
770119	331	48.74	52-40.77	148-45.04	59.99	3.51	7	270	117.7	0.29	11.6	5.1	D1
770304	927	54.85	53-17.58	147-47.21	94.00	3.75	15	72	75.3	0.38	2.3	4.5	B1
770314	745	5.03	52-51.77	149-37.12	80.93	4.50	15	50	102.8	0.12	1.9	5.8	C1
770505	1728	22.40	53-10.50	150-10.11	100.61	3.52	5	192	87.4	0.07	1.9	2.9	C1
770507	1556	45.15	52-23.71	149-35.75	78.11	3.85	5	230	152.9	0.11	4.9	7.7	D1
770515	1315	4.52	53- 2.99	149-29.22	39.57	4.10	8	175	157.1	0.31	4.3	432.8	D1
770725	1839	21.50	52-34.41	149-48.47	19.87	4.60	20	53	89.8	0.75	3.5	4.8	D1
780119	1424	43.51	53-10.57	149-51.09	94.28	3.85	22	52	77.0	0.33	1.5	3.8	B1
780402	1445	11.33	52-33.20	149-10.29	54.72	4.45	19	75	93.8	0.37	2.0	5.0	C1
780428	2132	5.27	53- 1.75	149-32.71	93.20	3.73	11	163	34.1	0.47	4.5	10.4	D1
780505	2243	52.18	52-30.58	149- 8.20	57.55	3.63	16	119	79.0	0.39	2.8	5.6	C1
780521	42	42.70	53- 3.05	149-13.33	80.73	3.55	17	149	77.3	0.37	2.5	5.4	D1
780510	1302	4.58	53- 0.41	149-13.42	59.05	4.25	22	90	82.2	0.39	2.0	3.3	C1
780525	1757	31.51	52-41.54	148-15.03	53.01	3.55	15	125	107.6	0.42	2.6	7.5	C1
780713	1524	50.05	52-53.27	149-35.25	59.00	3.54	22	50	99.9	0.41	2.2	4.0	C1
780715	1928	11.45	52-52.43	149-39.78	32.53	3.70	15	159	102.4	0.27	2.4	5.6	D1
780905	1650	6.34	53- 3.45	148-53.20	1.31	3.79	5	259	75.3	0.22	7.1	4.0	D1
780908	539	5.00	52-55.48	149-31.41	56.39	3.53	21	65	93.0	0.41	2.2	4.3	C1
780913	139	45.65	52-39.08	149-59.03	0.22	3.54	12	151	100.2	0.59	5.4	6.3	D1
780918	127	15.15	52-37.57	149-25.50	47.39	4.07	13	112	107.9	0.41	3.5	25.5	D1
780927	2150	2.85	52-35.80	149-57.59	28.53	3.80	9	175	121.8	0.69	7.9	14.3	D1
780329	2259	33.42	53- 7.15	149-35.91	91.71	3.62	9	197	76.3	0.34	5.1	8.6	D1
780909	2015	34.10	52-44.15	149-49.21	75.52	3.52	10	175	119.7	0.23	2.8	2.5	D1
780925	23 5	35.84	52-22.43	149-50.09	1.43	3.89	13	127	94.9	0.57	5.2	50.1	D1

REFERENCES

- Aki, K., 1965. Maximum Likelihood Estimate of b in the Formula $\log N = a - bM$ and its Confidence Limits, Bull. Earthquake Res. Inst., v. 43, pp. 237-239.
- Albanese, Mary, 1980. Recent Shallow Igneous Activity in the North Flank of the Central Alaska Range, Alaska, Unpublished M.S. thesis, Univ. of Alaska, Fairbanks.
- Anderson, John G., 1979. A Comment on the Relationship Between Earthquake Magnitude and Rupture Length, Earthquake Notes, v. 50, pp. 3-8.
- Bath, Markus, 1973. Introduction to Seismology, Halsted Press, N.Y.
- Barazangi, M., and B. L. Isacks, 1979. Subduction of the Nasca Plate Beneath Peru: Evidence from Spatial Distribution of Earthquakes, Geophys. J. R. Astr. Soc., v. 57, pp. 537-555.
- Beikman, Helen, 1974. Preliminary Geologic Map of Alaska, USGS Map and Chart Series MF-612.
- Berg, E., and H. Pulpan, 1971. Tilts Associated with Small and Medium Size Earthquakes, Jour. Phys. Earth, v. 19, pp. 59-78.
- Bhattacharya, B., and N. N. Biswas, 1979. Implications of North Pacific Plate Tectonics in Central Alaska: Focal Mechanisms of Earthquakes, Tectonophysics, v. 53, pp. 99-130.
- Biswas, N. N., 1973. P-Wave Travel-time Anomalies: Aleutian-Alaska Region, Tectonophysics, v. 19, pp. 361-367.
- Biswas, N. N., and B. Bhattacharya, 1974. Travel-time Relations for the Upper Mantle P-wave Phases from Central Alaskan Data, Bull. Seismol. Soc. Amer., v. 64, pp. 1953-1965.
- Bolt, B. A., J. Stifler, and R. Uhrhammer, 1977. The Briones Hills Earthquake Swarm of January 8, 1977, Contra County, California, Bull. Seismol. Soc. Amer., v. 67, pp. 1555-1564.
- Bolt, B. A., 1978. Incomplete Formulations of the Regression of Earthquake Magnitude with Surface Fault Rupture Length, Geology, v. 6, pp. 232-235.
- Boucher, Gary, T. Matumoto, and J. Oliver, 1968. Localized Micro-earthquakes in the Denali Fault Zone, Jour. Geophys. Res., v. 73, pp. 4789-4793.

- Boucher, Gary, and T. J. Fitch, 1969. Microearthquake Seismicity of the Denali Fault, *Jour. Geophys. Res.*, v. 74, pp. 6638-6648.
- Brew, D. A., R. A. Loney, and L.J.P. Muffler, 1966. Tectonic History of Southeastern Alaska, *Canadian Inst. of Mining and Metallurgy*, Special Vol. no. 8, pp. 149-170.
- Brogan, G. E., L. S. Cluff, M. K. Korrington, and D. B. Slemmons, 1975. Active Faults of Alaska, *Tectonophysics*, v. 29, pp. 73-85.
- Bufe, C. G., 1970. Frequency-Magnitude Variations During the 1970 Danville Earthquake Swarm, *Earthquake Notes*, v. 16, pp. 3-7.
- Cady, W. M., R. E. Wallace, T. M. Hoare, and E. J. Webber, 1955. The Central Kuskokwim Region, Alaska, *U.S. Geol. Surv. Prof. Paper* 268, 132 pp.
- Cox, D. R., and P.A.W. Lewis, 1966. The Statistical Analysis of Series of Events, Methuen and Company, Ltd., London, 285 pp.
- Davies, John, 1975. Seismological Investigations and Plate Tectonics in South-Central Alaska, Unpublished M.S. Thesis, University of Alaska, Fairbanks.
- Davies, J., and E. Berg, 1973. Crustal Morphology and Plate Tectonics in South-Central Alaska, *Bull. Seismol. Soc. Amer.*, v. 63, pp. 673-677.
- Davies, J. N., and L. House, 1979. Aleutian Subduction Zone Seismicity Volcano-Trench Separation, and Their Relation to Great Thrust-Type Earthquakes, *Jour. Geophys. Res.*, v. 84, pp. 4583-4591.
- Davis, T. Neil, 1964. Seismic History of Alaska and the Aleutian Islands. *Bibliographical Bull. Amer. Geophys. and Oceanography*, v. III, pp. 1-16 (Mexico).
- Davis, T. Neil, 1978. Report Summary: Operation of a Seismic Data Collection and Analysis Center in Alaska, in *Summaries of Technical Reports*, v. VII, National Earthquake Hazards Reduction Program, U.S.G.S., pp. 393-394.
- Davis, T. Neil, and Carol Echols, 1962. A Table of Alaskan Earthquakes, 1788 - 1961, *Geophysical Institute Research Report No. 8*, University of Alaska, Fairbanks.
- Engdahl, E. R., 1973. Relocation of Intermediate Depth Earthquakes in the Central Aleutians by Seismic Ray Tracing, *Nature Phys. Sci.*, v. 245, pp. 23-25.

- Estes, Steven, 1978. Unpublished M.S. Thesis, University of Alaska, Fairbanks.
- Forbes, R. B., D. L. Turner, J. Stout, and T. E. Smith, 1973. Cenozoic Offset Along the Denali Fault, Alaska (Abstract), EOS Trans. AGU, v. 54, no. 4, p. 495.
- Forbes, R. B., T. E. Smith, and D. L. Turner, 1974. A Solution to the Denali Fault Offset Problem, Alaska Div. Geol. and Geophys. Surveys Annual Report, 1973, pp. 25-27.
- Forbes, R. B., H. Pulpan, and L. Gedney, 1976. Seismic Risk and the Denali Fault, Part 1 - Tectonic History, Seismicity and the Development of Design Earthquakes and Computer Models, Geophysical Institute, Univ. of Alaska, October 1976.
- Gedney, Larry, 1970. Tectonic Stresses in Southern Alaska in Relationship to Regional Seismicity and the New Global Tectonics, Bull. Seismol. Soc. Amer., v. 60, pp. 1789-1802.
- Gedney, L., and E. Berg, 1969. Some Characteristics of the Tectonic Stress Pattern in Alaska, Geophys. J. R. Astr. Soc., v. 17, pp. 293-304.
- Grantz, A., 1966. Strike-slip Faults in Alaska, Ph.D. Thesis, Stanford University.
- Gutenberg, B., and C. F. Richter, 1944. Frequency of Earthquakes in California, Bull. Seismol. Soc. Amer., v. 34, pp. 185-188.
- Hanson, K., E. Berg, and L. Gedney, 1968. A Seismic Refraction Profile and Crustal Structure in Central Interior Alaska, Bull. Seismol. Soc. Amer., v. 58, pp. 1657-1665.
- Herrin, E., 1968. Seismological Tables for P, Bull. Seismol. Soc. Amer., v. 58, pp. 1196-1219.
- Hickman, R. G., and C. Craddock, 1973. Lateral Offsets Along the Denali Fault, Central Alaska Range, Alaska Geol. Soc. Amer., Abstracts with Programs, v. 7, p. 322.
- Hickman, R. G., C. Craddock, and K. W. Sherwood, 1978. The Denali Fault System and the Tectonic Development of Southern Alaska, Tectonophysics, v. 47, pp. 247-273.
- Huang, Paul, 1979. Aftershocks of the 1968 Rampart, Alaska, Earthquake, Unpublished M.S. Thesis, Univ. of Alaska, Fairbanks.
- Isacks, B., J. Oliver, and L. R. Sykes, 1968. Seismology and the New Global Tectonics, Jour. Geophys. Res., v. 73, pp. 5855-5896.

- Isacks, B., and P. Molnar, 1971. Distribution of Stresses in the Descending Lithosphere from a Global Survey of Focal-mechanism Solutions on Mantle Earthquakes, *Rev. Geophys. Space Phys.*, v. 9, p. 103.
- Jacob, K. H., K. Nakamura, and J. N. Davies, 1977. Trench-Volcano Gap Along the Alaska-Aleutian Arc: Facts and Speculations on the Role of Terrigenous Sediments for Subduction, in Talwani, M., and W. C. Pitman III, Editors, Island Arcs, Deep Sea Trenches and Back-Arc Basins, A.G.U., Washington, D.C.
- Kay, R. W., 1977. Geochemical Constraints on the Origin of Aleutian Magmas, in Talwani, M., and W. C. Pitman III, Editors, Island Arcs, Deep-Sea Trenches and Back-Arc Basins, Maurice Ewing Series 1, A.G.U., Washington, D.C.
- Kelleher, J., J. Savino, H. Rowlett, and Wm. McCann, 1974. Why and Where Great Thrust-Type Earthquakes Occur Along Island Arcs, *Jour. Geophys. Res.*, v. 79, pp. 4889-4899.
- Knopoff, L., and Y. Kagan, 1977. Analysis of the Theory of Extremes as Applied to Earthquake Problems, *Jour. Geophys. Res.*, v. 82, pp. 5647-5657.
- Lahr, J., and R. Page, 1972. Hypocentral Locations in the Cook Inlet Region of Alaska (Abstract), *EOS Trans. Amer. Geophys. U.*, v. 53, p. 1042.
- Lanphere, M. A., 1978. Displacement History of the Denali Fault System, Alaska and Canada, *Can. Jour. Earth Sci.*, v. 15, pp. 817-822.
- Lathram, E. H., 1964. Apparent Right-lateral Separation on the Chatham Strait Fault, Southeastern Alaska, *Bull. Geol. Soc. Amer.*, v. 75, pp. 249-252.
- Lee, W.H.K., and J. Lahr, 1971. HYP071: A Computer Program for Determining Hypocenter, Magnitude, and First Motion Pattern of Local Earthquakes, USGS Open-File Report.
- Lee, W.H.K., and S. W. Stewart, 1980. Principles and Applications of Microearthquake Nets, preprint, to appear in S. W. Smith (Editor), Advances in Geophysics - Methods of Experimental Geophysics, Academic Press, 345 p.
- Lomnitz, C., 1966. Magnitude Stability in Earthquake Sequences, *Bull. Seismol. Soc. Amer.*, v. 56, pp. 247-249.
- Loney, R. A., D. A. Brew, and M. A. Lanphere, 1967. Post-Paleozoic Radiometric Ages and their Relevance to Fault Movements, Northern Southeastern Alaska, *Bull. Geol. Soc. Amer.*, v. 78, pp. 511-526.

- Meyers, H., 1976. A Historical Summary of Earthquake Epicenters in and Near Alaska, NOAA Technical Memorandum EDS NGSDC - 1.
- Miller, T. P., and R. L. Smith, 1976. "New" Volcanoes in the Aleutian Volcanic Arc, in Cobb, E. H., Editor, The United States Geological Survey in Alaska: Accomplishments During 1975, Geological Survey Circular 733, p. 11.
- Minster, J. B., and T. H. Jordan, 1978. Present-Day Plate Motions, Jour. Geophys. Res., v. 83, pp. 5331-5354.
- Mogi, K., 1962. On the Time Distribution of Aftershocks Accompanying the Recent Major Earthquakes in and near Japan, Bull. Earthquake Res. Inst., v. 40, pp. 107-124.
- Page, Robert, 1968. Aftershocks and Microaftershocks of the Great Alaska Earthquake of 1964, Bull. Seismol. Soc. Amer., v. 58, pp. 1131-1168.
- Page, R. A., 1972. Crustal Deformation on the Denali Fault, 1942-1970, Jour. Geophys. Res., v. 77, pp. 1528-1533.
- Page, R., and J. Lahr, 1971. Measurements for Fault Slip on the Denali, Fairweather and Castle Mountain Faults, Alaska, Jour. Geophys. Res., v. 76, pp. 8534-8543.
- Plafker, G., 1965. Tectonic Deformation Associated with the 1964 Alaska Earthquake, Science, v. 148, pp. 1675-1687.
- Plafker, G., 1969. Tectonics of the March 27, 1964 Alaska Earthquake, U.S. Geol. Surv. Prof. Paper 543-I.
- Poppe, Barbara, 1979. Historical Survey of U.S. Seismograph Stations, U.S. Geol. Surv. Prof. Paper 1096.
- Pulpan, H., and J. Kienle, 1979. Western Gulf of Alaska Seismic Risk, Offshore Technology Conference Paper OTC 3612, pp. 2209-2213.
- Reed, B. L., and M. A. Lanphere, 1974. Offset Plutons and History of Movement Along the McKinley Segment of the Denali Fault System, Alaska, Bull. Geol. Amer., v. 85, pp. 1883-1892.
- Richter, Charles F., 1958. Elementary Seismology, Freeman Press, San Francisco.
- Richter, D. H., and N. A. Matson, Jr., 1971. Quaternary Faulting in the Eastern Alaska Range, Bull. Geol. Soc. Amer., v. 82, pp. 1529-1540.
- Rikitake, T., 1976. Earthquake Prediction, Elsevier Press, N.Y.

- Ringwood, A. E., 1974, The Petrological Evolution of Island Arc Systems, Jour. Geol. Soc. London, v. 130, pp. 193-204.
- Ryall, A., J. D. VanWormer, and A. E. Jones, 1968. Triggering of Microearthquakes by Earth Tides, and Other Features of the Truckee, California, Earthquake Sequence of September, 1966, Bull. Seismol. Soc. Amer., v. 58, pp. 215-248.
- St. Amand, Pierre, 1948. The Central Alaska Earthquake Swarm of October, 1947, Trans. Amer. Geophys. Union, v. 29, pp. 613-623.
- St. Amand, Pierre, 1954, The Tectonics of Alaska as Deduced from Seismic Data, Bull. Geol. Soc. Amer., v. 65, p. 1350 (Abstract).
- St. Amand, Pierre, 1957. Geological and Geophysical Synthesis of the Tectonics of Portions of British Columbia, the Yukon Territory, and Alaska, Bull. Geol. Soc. Amer., v. 68, pp. 1343-1370.
- Sainsbury, C. L., and W. S. Twenhofel, 1954. Fault Patterns in Southeastern Alaska, Bull. Geol. Soc. Amer., v. 65, p. 1300 (Abstract).
- Savage, J. C., 1975. Further Analysis of the Geodetic Strain Measurements on the Denali Fault in Alaska, Jour. Geophys. Res., v. 80, pp. 3786-3790.
- Savage, William U., 1976. Earthquake Probability Models: Recurrence Curves, Aftershocks and Clusters, Technical Report, Seismological Laboratory, Univ. of Nevada.
- Scholz, C. H., 1968. The Frequency-Magnitude Relation of Microfracturing in Rock and its Relation to Earthquakes, Bull. Seismol. Soc. Amer., v. 58, pp. 399-415.
- Schwarz, W. M., R. N. Anderson, and S. E. DeLong, 1977. A Thermal Model for Subduction with Dehydration in the Down-going Slab (Abstract), EOS, v 58, p. 500.
- Smith, T. E., 1971. Geology, Economic Geochemistry, and Placer Gold Resources of the Western Clearwater Mountains, East-central Alaska, Ph.D. Thesis, Univ. of Nevada, Reno.
- Smith, T. E., and M. A. Lanphere, 1971. Age of the Sedimentation, Plutonism, and Regional Metamorphism in the Clearwater Mountains Region, Central Alaska, Isochron/West, no. 2, pp. 17-20.
- Stauder, W., and G. A. Bollinger, 1966. The Focal Mechanism of the Alaska Earthquake of March 28, 1964, and its Aftershock Sequence, Jour. Geophys. Res., v. 71, pp. 5283-5296.

- Stout, J. H., 1965. Bedrock Geology Between Rainy Creek and the Denali Fault, Eastern Alaska Range, Alaska, Unpublished M.S. Thesis, Univ. of Alaska, Fairbanks, 77 pp.
- Stout, J. H., J. B. Brady, F. Weber, and R. A. Page, 1973. Evidence for Quaternary Movement on the McKinley Strand of the Denali Fault in the Delta River Area, Alaska, *Bull. Geol. Soc. Amer.*, v. 84, pp. 939-948.
- Sykes, L. R., 1971. Aftershock Zones of Great Earthquakes, Seismicity Gaps, and Earthquake Prediction for Alaska and the Aleutians, *Jour. Geophys. Res.*, v. 76, pp. 8021-8041.
- Tatel, H. E., and M. A. Tuve, 1956. Seismic Crustal Measurements in Alaska, (Abstract), *Trans. Amer. Geophys. Union*, v. 37, p. 360.
- Thatcher, W., and T. C. Hanks, 1973. Source Parameters in Southern California Earthquakes, *Jour. Geophys. Res.*, v. 78, pp. 8547-8576.
- Tobin, D. G., and L. R. Sykes, 1966. Relationship of Hypocenters of Earthquakes to the Geology of Alaska, *Jour. Geophys. Res.*, v. 71, pp. 1659-1667.
- Tobin, D. G., and L. R. Sykes, 1968. Seismicity and Tectonics of the Northeast Pacific Ocean, *Jour. Geophys. Res.*, v. 73, pp. 3821-3845.
- Twenhofel, W. S., and C. L. Sainsbury, 1958. Fault Patterns in South-eastern Alaska, *Bull. Geol. Soc. Amer.*, v. 69, pp. 1431-1442.
- Utsu, T., 1965. A Method of Determining the Value of b in a Formula $\log N = a - bM$ Showing the Magnitude-Frequency Relation for Earthquakes (in Japanese with English abstract), *Geophysical Bulletin, Hokkaido Univ., Japan*, v. 13, pp. 99-103.
- Utsu, T., 1969. Aftershocks and Earthquake Statistics, (I) - Some Parameters Which Characterize an Aftershock Sequence and their Interrelations, *Jour. Faculty Sci., Hokkaido Univ., Japan, Series VII*, v. III, pp. 129-195.
- VanWormer, D., J. Davies, and L. Gedney, 1973. Central Alaska Earthquakes During 1972, Univ. of Alaska Geophysical Institute Scientific Report UAG R-224.
- VanWormer, D., J. Davies, and L. Gedney, 1974. Seismicity and Plate Tectonics in South-Central Alaska, *Bull. Seismol. Soc. Amer.*, v. 64, pp. 1467-1475.

- VanWormer, J. D., L. Gedney, J. N. Davies, and N. Condal, 1975.
Vp/Vs and B-values: A Test of the Dilatancy Model for Earth-
quake Precursors, Geophys. Res. Letters, v. 2, pp. 514-516.
- Wyss, M., 1979. Estimating Maximum Expectable Magnitude of Earth-
quakes from Fault Dimensions, Geology, v. 7, pp. 336-340.
- Wyss, M., and W.H.K. Lee, 1973. Time Variations of the Average
Earthquake Magnitude in Central California, Stanford Univ.
Pub. Geol. Soc., v. 13, pp. 24-42.
- Wahrhaftig, C., D. L. Turner, F. R. Weber, and T. E. Smith, 1975.
Nature and Timing of Movement on Hines Creek Strand of Denali
Fault System, Alaska, Geology, August, pp. 463-466.